Analysis of *Map3k*-dependent molecular mechanisms regulating signaling in iNKT and B cells

Saba Anwar

Molecular Biology Master's Thesis (60 Cr)

June 2013

Project Supervisor: Dr Ewen Gallagher (Imperial College London)

Abstract

Our immune system consists of two types of lymphocytes; B lymphocytes which produce antibodies in response to an antigen, and T lymphocytes which differentiate into particular effector T lymphocytes such as a cytotoxic, helper or regulatory T cell in response to an antigen. Type 1 invariant natural killer T cells (iNKT cells) are a unique population of T cells whose phenotypical, developmental and functional characteristics differ from conventional T cells (Novak and Lehuen, 2011). Mitogen-Activated Protein Kinase (MAPK) signaling is critical for T lymphocyte development and effector responses. We define the roles of *Map3k1* and *Map3k7* genes in Natural Killer T (NKT) cells. We identify an elevated expression of the cell cycle inhibitor *Cdkn1b* during the *Map3k1*$^{\Delta KD}$ iNKT cell clonal burst. We find aberrant Interleukin (IL) -17 production by *Map3k1*$^{\Delta KD}$ iNKT cells and altered expression of *Rorc*, *Mmp9* and *Il17rb* in *Map3k1*$^{\Delta KD}$ iNKT cells. The liver damage seen in *Map3k1*$^{\Delta KD}$ mice could be the cause of upregulation of Il-17 and IL-1β cytokines, and IL-1β related genes (*Il1r2 and Il1f9*). Additionally we find that *Map3k1*$^{+/\Delta KD}$ mice injected with keyhole limpet hemocyanin (KLH) display a larger population of germinal center B cells compared to *Map3k1*$^{\Delta KD}$ mice suggesting an importance of *Map3k1* in germinal center formation.

Abbreviations

αGal-Cer – α-Galactoceramide

APC – Antigen Presenting Cell

BAFF – B-cell Activating Factor

BCR – B Cell Receptor

BrdU - Bromodeoxyuridine

BSA – Bovine Serum Albumin

C57BL/6 - C57 black 6

Cdkn1b - Cyclin-dependent kinase inhibitor 1B

cDNA – complementary Deoxyribonucleic Acid

cRNA – complementary Ribonucleic Acid

Ct – Cross threshold

Cxcr2 - Chemokine (C-X-C motif) receptor 2

DC – Dentritic Cell

D-CDK4 - Cyclin-Dependent Kinase 4

dNTP - Deoxyribonucleotide triphosphate

EAE - Experimental Autoimmune Encephalomyelitis

E-CDK2 - Cyclin-Dependent Kinase 2

EDTA - Ethylenediaminetetraacetic acid

EGr2 – Early Growth response 2

ELISA – Enzyme Linked Immunosorbent Assay

ERK – Extracellular Signal Regulated Kinase

ES cell – Embryonic Stem cell

FACS - Fluorescence-Activated Cell Sorting

FBS – Foetal Bovine Serum

Flp - Flippase

FO – Follicular

Foxp3 - Forkhead box P3

FRT - Flippase Recognition Target

G_1 phase – Growth 1 phase

G_2 phase – Growth 2 phase

GM-CSF – Granulocyte Macrophage-Colony Stimulating Factor

H&E - Hematoxylin and Eosin

ICC – Intracellular Cytokine Staining

IFN – Interferon

Ig – Immunoglobulin

iNKT – Invariant Natural Killer T

i.p. - Intraperitoneal

JNK – c-Jun N-terminal Kinase

KLH – Keyhole Limpet Hemocyanin

Lck – Lymphocyte protein tyrosine kinase

Loxp - Locus of X-over P1

LPS - Lipopolysaccharide

MACS – Magnetic Activated Cell Sorting

MAPK - Mitogen Activated Protein Kinase

MAPKK – Mitogen Activated Protein Kinase Kinase

MAPKKK - Mitogen Activated Protein Kinase Kinase Kinase

MHC – Major Histocompatibility Complex

Mmp9 - Matrix metallopeptidase 9

mRNA – messenger Ribonucleic Acid

MZ – Marginal Zone

Neo - Neomycin

NFAT - Nuclear factor of activated T-cells

NF-κB – Nuclear Factor Kappa-light-chain-enhancer of activated B cells

NIK - NF-κB–Inducing Kinase

P27 - Cyclin-dependent kinase inhibitor 1B

PBMC – Peripheral Blood Mononuclear Cell

PBS – Phosphate Buffer Solution

PCR – Polymerase Chain Reaction

PKCϴ – Protein Kinase C ϴ

PSG – Penicillin Streptomycin Glutamine

qRT-PCR - quantitative Reverse Transcription Polymearase Chain Reaction

RBC – Red Blood Cell

RORC – RAR-Related Orphan Receptor C

RORγ – RAR-Related Orphan Receptor Gamma

S phase – Synthesis phase

SAP – SLAM Associated Protein

SAPK – Stress Activated Protein Kinase

SEM – Standard Error of the Mean

SLAM - Signaling Lymphocyte-Activation Molecule

STAT3 - Signal Transducer and Activator of Transcription 3

SV40 poly A - Simian virus 40 PolyA

TAK1 - Transforming growth factor β activated kinase-1

TCR – T Cell Receptor

TD – Thymus Dependent

TGF –Transforming Growth Factor

Th – T helper

TI-1 – Thymus Independent Type 1

TI-2 – Thymus Independent Type 2

TMB – Tetramethylbenzidine

TNF – Tumour Necrosis Factor

TNFR – Tumour Necrosis Factor Receptor

Introduction

The cells of our immune system arise from a pluripotent hematopoietic stem cell in the bone marrow, which divide to produce a common lymphoid progenitor and a common myeloid progenitor. It is the common lymphoid progenitor that gives rise to the lymphoid lineage of leukocytes which includes natural killer (NK) cells and T and B cells (Fig.1). T cells mediate our adaptive immune system. An adaptive immune response is triggered when pathogens overcome the innate defence mechanisms. T cells undergo development in the thymus and once their development is complete they enter the bloodstream. Once they arrive at a peripheral lymphoid organ they leave the blood to migrate through the lymphoid tissue returning by the lymphatic system to the bloodstream to re-circulate between the blood and peripheral lymphoid tissues. A naive T cell is one that has not yet encountered their specific antigen. To participate in an adaptive immune response a naive T cell must come across its specific antigen, present itself as a peptide: MHC complex on the surface of an antigen presenting cell and be induced to proliferate and differentiate into effector T cells. CD8 T cells recognize pathogen peptides presented by major histocompatibilty complex (MHC) class I molecules, naive CD8 T cells differentiate into cytotoxic effector T cells that recognize and kill infected cells. CD4 T cells recognize pathogen peptides presented my MHC class II molecules. Naive CD4 T cells can differentiate down different pathways that produce effector subsets with different immunological functions. The main CD4 effector subsets are Th1 cells which activate infected macrophages and also provide help to B cells for antibody production, Th2 cells, which provide help to B cells for antibody production, especially switching to IgE and Th17 cells which enhance neutrophil response and promote barrier integrity (Murphy., 2011).

iNKT cells

Type 1 invariant natural killer T (iNKT) cells are a unique population of T cells whose phenotypical, developmental and functional characteristics differ from conventional T cells (Novak and Lehuen, 2011). iNKT cells are restricted by CD1d, a family of MHC like molecules that specialize in presenting lipid antigens to T cells. iNKT cells express a highly restricted T cell receptor (TCR), a majority of iNKT cells express the Vα14Jα18 chains with a restricted set of β chains Vβ8.2, Vβ7 and

Vβ2 in mice. Type 1 NKT cells are detected with glycolipid α-galactosylceramide (α-GalCer) loaded CD1d tetramers. CD1d is constitutively expressed by antigen presenting cells (APCs) such as dentritic cells (DCs), macrophages and marginal zone (MZ) B cells. CD1d is also expressed on cortical thymocytes where it is necessary for NKT cell development, and on Kupffer cells and endothelial cells lining liver sinusoids where the highest frequency of NKT cells are found in mice (Bendelac et al., 2007). iNKT cells in mice contribute approximately 0.5% of the T cell population in the blood and peripheral lymph nodes, 2.5% of T cells in the spleen, mesenteric and pancreatic lymph nodes and up to 30% of T cells in the liver (Bendelac et al., 2007).

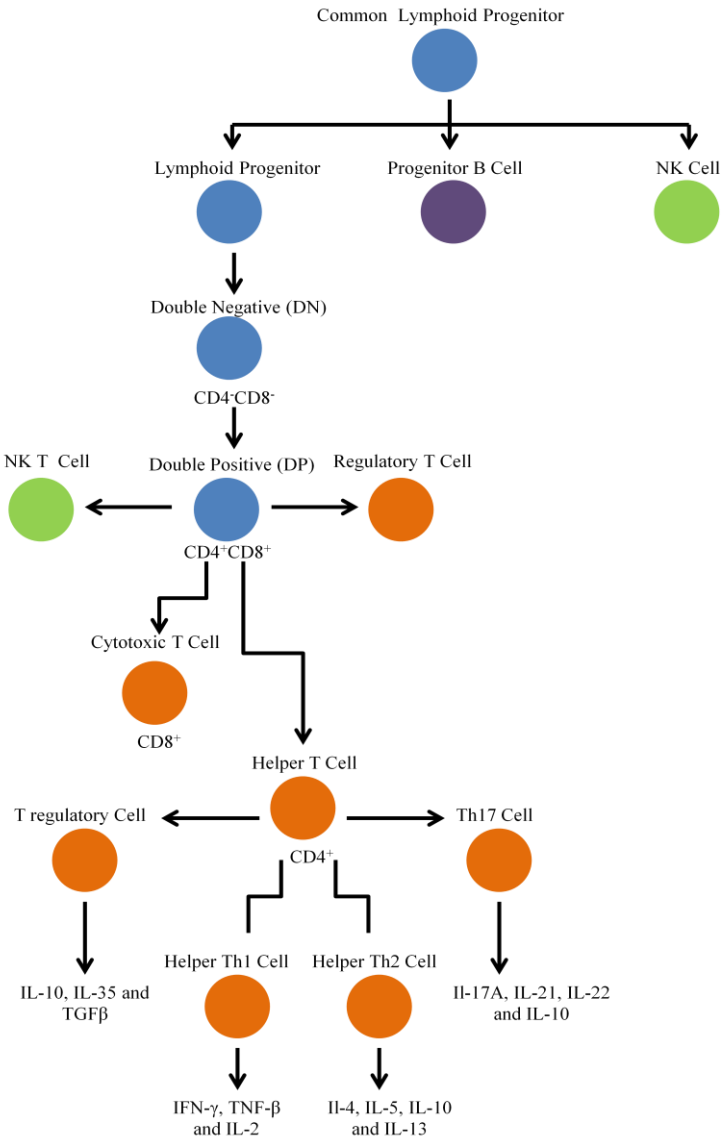

Fig 1: T cell development. The diagram shows the differentiation process that occurs to a common lymphoid progenitor. A common lymphoid progenitor in the bone marrow gives rise to the lymphoid lineage of leukocytes – the NK cells and the T and B lymphocytes.

iNKT cells have many functions *in vivo,* during an immune response they have the ability to secrete a variety of cytokines within a few hours after activation such as IFN-γ, IL-4, IL-2, IL-5, IL-6, IL-10, IL13, Il-17, IL-21, TNF-α, TGF-β and GM-CSF with production of IL-4 and IFN-γ being a signature feature of iNKT cells following α-GalCer antigen administration. iNKT cells express high levels of granzyme B, perforin and FasL giving iNKT cells a cytolytic property. iNKT cells also have the capacity to influence other cells of the immune system. Studies have shown that iNKT cell derived cytokines can activate several other cell types including NK cells, conventional $CD4^+$ and $CD8^+$ T cells, macrophages and B cells (Matsuda et al., 2008).

Development of iNKT cells occurs in the thymus. iNKT cells diverge from conventional T cells during development at the double positive thymocyte stage which is concurrent with TCRβ expression (Matsuda et al., 2008). iNKT cell development needs the recognition of self and it has been shown that iNKT cells are selected at the double positive stage by CD1d expressing $CD4^+CD8^+$ double positive thymocytes (Gapin et al., 2001). iNKT cells expand in the thymus once they have been positively selected. They undergo an organized maturation process that leads to the acquirement of their activated NK-like phenotype. Most iNKT cells leave the thymus in an immature stage (lacking expression of NK receptors) and complete their end maturation in the periphery (Matsuda et al., 2008).

Th17 cells

Th17 cells are a distinct lineage of pro-inflammatory T helper cells that are essential in autoimmune disease (Wilson et al., 2007). Th17 cells can protect the host against extracellular pathogens encountered at mucosal surfaces, and Th17 cells also play roles in multiple sclerosis, liver inflammation, inflammatory bowel disease, and psoriasis (Ouyang et al., 2008; Patel et al., 2007). Th17 cells secrete numerous cytokines such as IL-17A, IL-17F and IL22 (Zhou and Littman, 2009). IL-17 activity plays a role in acute inflammation. The IL-17 mediated release of IL-6 and IL-8 from mesenchymal cells leads to fever, an acute phase response (increase in levels in plasma proteins) and the accumulation of neutrophils in blood and tissue. IL-17 activity also contributes to chronic

inflammation which can be linked with matrix destruction. IL-17 induces an inhibitory effect on matrix production in chondrocytes and osteoblasts which leads to joint damage and defective tissue repair (Miossec and Kolls, 2012). In mice, Transforming Growth Factor (TGF) -β and IL-6 cause the differentiation of T-cells into Th17 cells by inducing the expression of a transcription factor called retinoic acid receptor-related orphan nuclear receptor RORγt (encoded by Rorc) and the IL-23 receptor (Ivanov et al., 2006; Veldhoen et al., 2006; Zhou and Littman, 2009).

B cells

B cells are a component of the innate and adaptive immune system. B cells posses several functions, they are specialized APCs that contribute to the activation/amplification of naive, activated and autoreactive T cell responses. B cells can produce different proinflammatory cytokines such as TNFα, IFNγ and IL-12 that are a feature of responses by B effector type 1 cells which are associated with Th1 responses. B effector type 2 cells produce IL-4 and IL-13 cytokines associated with Th2 responses (Mauri, 2010). Both subsets make IL-2, IL-6 and IL-10 (Gray et al., 2007). B cells have the ability to initiate B cell proliferation, differentiation and antibody secretion to any of the three types of antigens – thymus independent type 1 (TI-1), thymus independent type 2 (TI-2) and thymus dependent (TD). B cells will go through different differentiation pathways depending on the type of antigen which has activated them. A B cell reacting to a TD antigen and CD40 ligand matures in the germinal centre and can somatically mutate and give rise to memory and plasma cells. A TI-2 responding cell produces IgM, with no memory and little or no somatic mutation. TI-2 antigens cause multivalent cross linking of the B cell receptor (BCR); however there is a need for additional signals provided by noncognate interaction with T cells, NK cells and possibly other cell types. This leads to the production of IgM and some IgG3 antibodies containing few or no somatic mutations. Long term memory cells are not generated (Berland and Wortis, 2002).

B cells arise from a common lymphoid progenitor and differentiate into several B cell types (Fig.2), such as plasma B cells, memory B cells, follicular (FO) B cells, MZ B cells, regulatory B cells, B-1 and B-2 B cells. Plasma cells are B cells that secrete a large amount of antibodies on contact with an

antigen. Antibodies function both as a natural barrier to infection and as a humoral component of adaptive immune responses to pathogens (Bouaziz et al., 2008). Marginal zone B cells are found at the border of the white and red pulps of the spleen. They are able to respond rapidly to antigenic challenge involving metallophilic macrophages and dentritic cells. MZ B cells go through rapid migration to lymphoid follicles after contact with bacterial products, this helps to transport systemic antigens to follicular dentritic cells. MZ B cells are involved in T cell independent responses (Viau and Zouali, 2005). FO B cells are involved in T cell dependent antibody responses and generating plasma and memory cells (Viau and Zouali, 2005). B-1 B cells are a small subpopulation of B cells found in the pleural and peritoneal cavities, spleen and parts of the intestine. B-1 B cells are mediators of the innate immune system. When exposed to specific pathogens B-1 B cells are activated and secrete 'natural antibodies' which are usually of the IgM class that bind to T-cell independent antigens (Montecino-Rodriguez et al., 2006). B-2 (conventional) B cells are the major population of B cells present in the spleen and lymph nodes. They are produced in the bone marrow and function primarily in the adaptive immune response (Montecino-Rodriguez et al., 2006). Memory B cells occupy the spleen, and lymph nodes and can also be found circulating through the blood. Memory B cells are produced from mature B cells after their first encounter to an antigen. On subsequent exposure to the same antigen memory B cells respond rapidly by secreting antibodies (Murphy., 2011). Regulatory B cells are a phenotypically unique and rare subset of B cells. They are recognized by their $CD1d^{hi}CD5^{+}$ phenotype and their ability to produce and secrete IL-10. Regulatory B cells have the ability to influence T cell activation and some inflammatory responses (Bouaziz et al., 2008).

Fig. 2. B cell development. B cells derive from a common lymphoid progenitor cell which gives rise to the pro-B cell, the earliest committed B-lineage cell. B cell development begins in primary lymphoid tissues with maturation occurring in secondary lymphoid tissues.

MAPK signaling pathway

MAP kinases are major components of pathways controlling embyogenesis, cell differentiation, cell proliferation and cell death (Pearson et al., 2001). In mammals four main groups of MAPKs have been found: extracellular signal regulated kinases (ERKs) 1 and 2 (ERK1/2), c-Jun amino terminal

kinases or stress activated protein kinases (JNK/SAPK) 1-3, p38MAPKα, β, γ and δ and ERK5. Most of the information known about these groups comes from the study of three groups of MAPKs : ERK1/2, JNK1/2 and p38 MAPK (Aouadi et al., 2006). MAP kinases are regulated by phosphorylation cascades, the phosphorylation events that comprise such cascades target the activation loop which is a structural feature common to all protein kinases. Phosphorylation of the activation loop leads to a conformational switch which enables the catalytic site to be accessible to ATP and protein substrates. Each MAPK family is composed of three modules activated on series and leading to the activation of specific MAP kinase: a MAP kinase kinase (MAPKK) represented by MEK or MKK proteins which phosphorylates a specific MAPK and a MAP kinase kinase kinase (MAPKKK) represented by Raf and MEKK proteins which phosphorylates a specific MAPK (Fig.3) (Aouadi et al., 2006). MEKK1 is a member of the MAPK kinase (MAP2K) kinase (MAP3K) family that regulate JNK and p38 MAPKS by phosphorylation of MAP2Ks activation loop (Karin and Gallagher, 2005; Matsuzawa et al., 2008). *Map3k1*$^{\Delta KD}$ B cells have intrinsic JNK and p38 signaling defects from Tumour Necrosis Factor (TNF) Receptor family members (TNFRs) CD40 and B cell activating factor belonging to the TNF family (BAFF) receptors (Matsuzawa et al., 2008). Similarly, another member of the MAP3K family, TGF-β Activated Kinase -1 (TAK1, encoded by *Map3k7*) is important in innate and adaptive immune signaling cascades (Ninomiya-Tsuji et al., 1999; Wang et al., 2001). TAK1 is activated in response to TNF family cytokines and by lipopolysaccaride (LPS), and is involved in controlling the activation of p38, JNK and NF-κB in several cellular systems (Rincon and Davis, 2009).

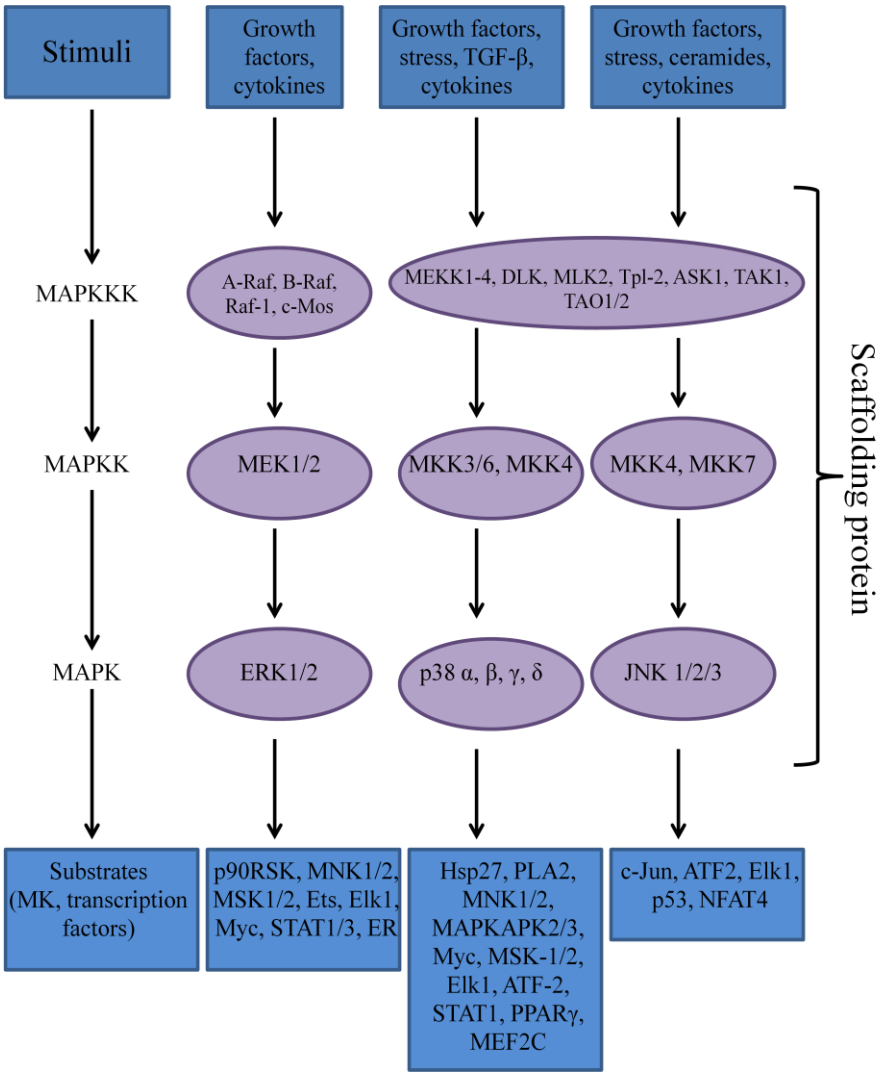

Fig 3. MAPK pathways. In mammals at least four different groups of MAPKs have been found : extracellular signal regulated kinases (ERKs) 1 and 2 (ERK1/2), c-Jun amino terminal kinases or stress activated protein kinases (JNK/SAPK) 1-3, p38MAPKα, β, γ and δ and ERK5. Most of the information known about these groups comes from the study of three groups of MAPKs : ERK1/2, JNK1/2 and p38MAPK. These serine/threonine kinases are regulated by phosphorylation cascades organized in specific modules. Each MAPK family is composed of three modules activated on series and leading to the activation of specific MAP kinase : a MAP kinase kinase (MAPKK) represented by MEK or MKK proteins which phosphorylates a specific MAPK and a MAP kinase kinase kinase (MAPKKK) represented by Raf and MEKK proteins which phosphorylates a specific MAPKK. MAPK cascades are organized in complexes by scaffolding proteins that contribute to their specificity and localization.
Abbreviations: ATF, activating transcription factor; ASK, Apoptosis Signal–regulating Kinase; DLK, dual leucine zipper-bearing kinase; ER, estrogen receptor; ERK, extracellular signal-regulated kinase; hsp27, small heat shock protein 27; JNK, c-Jun amino-terminal kinase; MAPKAP, MAP kinase-activated protein kinase; MEF, myocyte-enhancing factor; MEK, MAP/ERK kinase; MEKK, MEK kinase; MLK, mixed-lineage protein kinase; Mnk, MAP kinase-interacting kinase; Msk, mitogen- and stress-activated protein kinase; NFAT4, Nuclear factor of activated T cells 4; PLA2, phospholipase A2; PPAR, peroxisome proliferative-activated receptor; Rsk, ribosomal S6 kinase; STAT, signal transducer and activator of transcription; TAK, transforming growth factor activated-β-protein kinase; TAO, one thousand and one amino acids. (Aouadi et al., 2006)

In this research study, we have investigated the molecular roles of *Map3k1* and *Map3k7* in relation to iNKT cells. We have shown that *Map3k1* and *Map3k7* differentially control iNKT cell expansion through distinct mechanisms. *Map3k1*$^{+/\Delta KD}$ and *Map3k1*$^{\Delta KD}$ iNKT splenic cells have been characterized through microarray genetic profiling to understand the molecular basis of the iNKT cell defect triggered by the absence of *Map3ks*. An increase in the cell cycle inhibitor p27 offers an explanation for the *Map3k*-dependent proliferative expansion seen in iNKT cells. An upregulated expression of Th17 related genes *Rorc*, *Mmp9* and *Il17rb* in *Map3k1*$^{\Delta KD}$ iNKT cells has also been identified suggesting an association between the Th17 differentiation pathway and the *Map3k1*$^{\Delta KD}$ iNKT cells. IL-17RB^{+} iNKT cells may also play a role in the underlying iNKT cell cytokine production defect present within *Map3k1*$^{\Delta KD}$ mice. In addition, enhanced expression of IL-17 and IL-1 cytokines could account for the enhanced liver damage observed in *Map3k1*$^{\Delta KD}$mice.

Conditional *Map3k1* mice have been generated in our group using a strategy of site-specific recombination. In our *Map3k1*^{flox} mouse, a critical exon of the *Map3k1* gene is flanked by FRT sites and loxP sites. When the *Map3k1* flox mouse is crossed with *Flpe* mice, there will be a site-specific recombination at the FRT sites, creating a floxed allele. A floxed mouse is used to describe a genetically manipulated mouse that has a specific DNA sequence between two loxp sites. Recombination between loxP sites is catalysed by Cre recombinase. Floxing a gene allows it to be deleted (knocked out), translocated or inverted. Floxed genes can be used to produce tissue-specific knockouts. For example, in our case, we will be using two different Cre recombinase mice, the CD19-Cre and Lck-cre mice that will cause the floxed *Map3k1* to be inactivated in B and T cells respectively. If Cre expression occurs without Flp expression, a reporter knockout mouse will be generated which possesses a LacZ gene. Keyhole limpet hemocyanin (KLH) stimulates B cells; a study has shown that after 10 day immunization of *Map3k1*$^{\Delta KD}$ and *Map3k1*$^{+/\Delta KD}$ with KLH, spleens from *Map3k1*$^{+/\Delta KD}$ mice had a larger population of germinal centre B cells positive for the GL7 marker of activated B cells compared to *Map3k1*$^{\Delta KD}$ mice (Gallagher et al., 2007). Stimulating B cells using KLH in the *Map3k1* flox conditional system will allow us to investigate how silencing the

Map3k1 gene in B cells will influence protein signaling and the immune responses in those cells. We will able to assess differences in protein and cellular expression between *Map3k1*^{flox} and control mice.

Materials and Methods

Generation of *Map3k1*$^{\Delta kd}$ and *Lck-Cre*$^{+}$*Map3k7*$^{f/f}$ mice

The research group performed experiments using the *Map3k1*$^{\Delta KD}$ mice. This genetically modified knockout *Map3k1*$^{\Delta KD}$ mouse strain was previously generated using a targeting vector (Fig 4) to disrupt the *Map3k1* locus in mouse ES cells. Incorporation of the targeting vector into the *Map3k1* locus leads to the generation of a *Map3k1*-β-galactosidase fusion protein containing the first 1188 amino acids of *Map3k1* however deficient of its entire kinase domain. Homozygote double negative *Map3k1* knockout mice will be denoted as *Map3k1*$^{\Delta KD}$ and heterozygote single positive control *Map3k1* knockout mice will be denoted as *Map3k1*$^{+/\Delta KD}$ throughout the paper. *Lck-Cre*$^{+}$ and *Map3k7* mice bought from The Jackson Laboratory, were previously crossed to generate *Lck-Cre*$^{+}$*Map3k7*$^{f/f}$ mice for ongoing research. Homozygote double negative *Map3k7* knockout mice will be denoted as *Lck-Cre*$^{+}$*Map3k7*$^{f/f}$ and heterozygote single positive control *Map3k7* knockout mice will be denoted as *Lck-Cre*$^{+}$*Map3k7*$^{+/f}$ throughout the paper. The mice were bred and maintained under pathogen free conditions in conventional barrier protection and in accordance with the guidelines of Imperial College London and mouse protocols approved by the Home Office (London, UK). 2μg of KRN7000 (Enzo Life Sciences) an analogue of α-GalCer and a specific ligand for human and mouse NKT cells, was injected i.p. to mice that were 4 and 6 weeks old. For B cell stimulation, mice were immunized i.p. with 100μg KLH precipitated in alum.

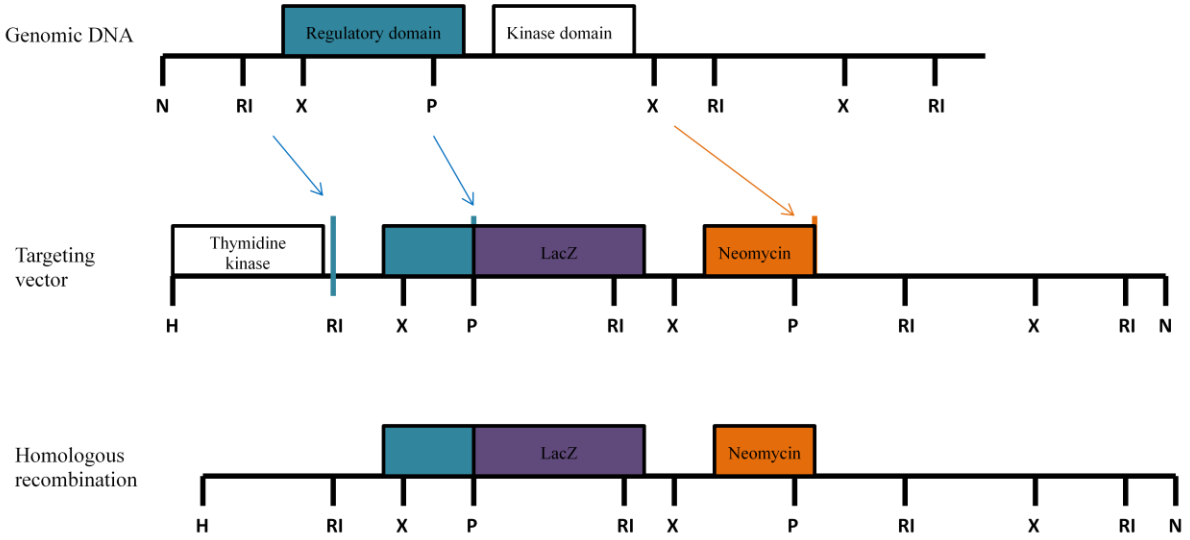

Figure 4: Diagram of targeting strategy used to generate *Map3k1*^{KD} ES cells. Schematic structures of the *Map3k1* locus, the targeting vector, and the homologous recombinant and positions of the N-terminal regulatory region, C-terminal catalytic kinase domain of *Map3k1*, restriction sites (H=HindIII; RI=EcoRI; P=Pstl; N=Notl;X=Xbal;B=BamHI), positive selection marker neomycin and negative selection marker thymidine kinase. Disruption of *Map3k1* locus due to substitution of the exons coding for the Map3k1 kinase domain with the bacterial *LacZ* gene, generating a Map3k1^{KD} allele which specifies the expression of a *Map3k1* –β-galactosidase fusion protein containing the first 1188 amino acids of *Map3k1* but lacking the kinase domain.

The research group have been in the process of generating *Map3k1*^{loxP}. This was initiated by obtaining *Map3k1*^{flox} mice, maintained on a C57BL/6 background, from the Sanger Institute. A cassette was inserted in chromosome 13 upstream of the critical exon in *Map3k1* (Fig. 5). The cassette is composed of an FRT site followed by a LacZ sequence and a loxP site. The first loxP site is followed by neomycin under the control of the human B-actin promoter, SV40 poly A, a second FRT site and a second loxP site. A third loxP site is inserted downstream of the targeted exon. *Map3k1*$^{+/flox}$ mice crossed with ACTFLPe mice will cause recombination at the FRT sites, deletion of the *lacZ* and neo marker sites, and will result in offspring with a conditional *Map3k1*^{loxP} allele through *flp* recombinase expression. To produce mice with tissue specific *Map3k1* deletion, we subsequently cross the *Map3k1*^{loxP} homozygote mice with either CD19-Cre or Lck-cre mice.

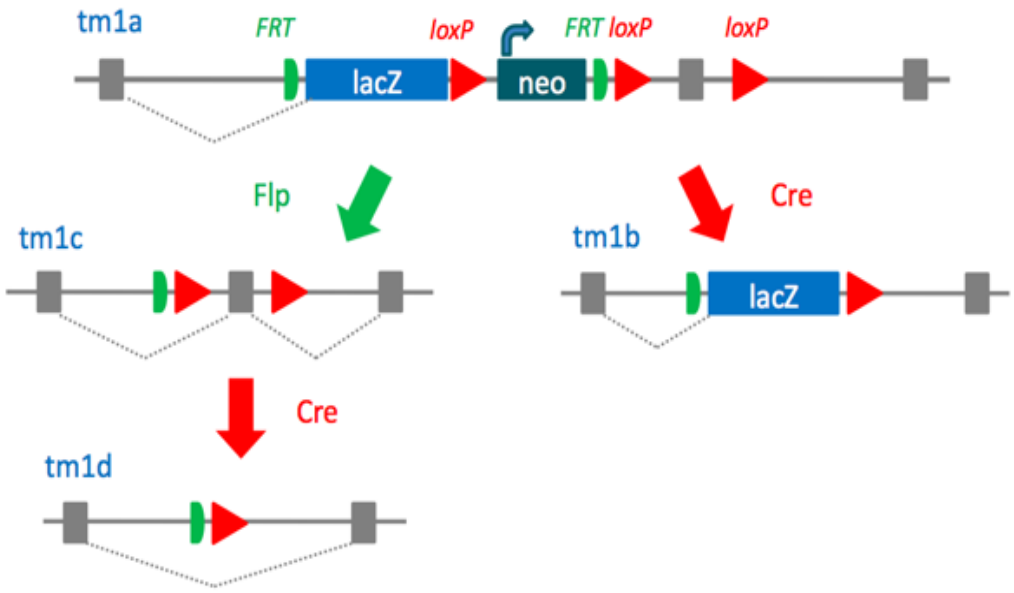

Figure 5: Diagram of targeting strategy used to generate *Map3k1*^{flox} mice. Insertion of a cassette composed of an FRT site, followed by lacZ and loxP site at chromosome 13. The first loxP site is followed by neomycin under the control of the human β-actin promoter, SV40 polyA, a second FRT site and a second loxP site. A third loxP site is inserted downstream of the targeted exon. *Map3k1*$^{+/flox}$ mice crossed with ACTFLPe mice will cause recombination at the FRT sites, deletion of the lacZ and neo marker sites, and will result in offspring with a conditional *Map3k1*^{loxP} allele through flp recombinase expression. Mice with deletion of *Map3k1* in specific tissues will be generated following Cre-recombinase activity.

Currently this site specific recombination in *Map3k1*^{flox} mice is still under progress. So far the work done has involved crossing *Map3k1*^{flox} mice with FLPe mice which would cause site specific recombination at the FRT sites in the *Map3k1*^{flox} mice and the deletion of the LacZ sequence. The F1 mice generation were biopsied and polymerase chain reaction (PCR) was carried out to check whether the correct genotype was obtained. Once assured that the mutant gene was present on both alleles to produce homozygote mice, the next step for the research group would be to cross the manipulated conditional *Map3k1*^{loxP} mice with either CD19-Cre or Lck-cre mice to silence the gene expression in specific tissues.

Genotyping

Genotyping was carried out on two strains of mice *Map3k1*^{loxP} and *Lck-Cre*$^{+}$*Map3k7* mice. For *Lck-Cre*$^{+}$*Map3k7* mice, PCR was carried out for *Map3k7* and *Lck-Cre* using appropriate primers. For the generation of *Map3k1*^{loxP} mice, PCR was carried out for *Map3k1*, *LacZ* and *FLPe* to ensure obtaining correct sized band. PCR was carried out using Extract-N-Amp Tissue PCR kit (Sigma). Water, Extract-N-Amp PCR reaction mix, forward primer and reverse primer and tissue extract was added to a total volume of 20µl. A general thermal cycling protocol (table 1) was used however adjusted according to different primers.

Table 1: Common cycling parameters

Step	Temperature (ºC)	Time (minutes)	Cycles
Initial denaturation	94	3	1
Denaturation	94	0.5-1	30-35
Annealing	45-68	0.5-1	
Extension	72	1-2	
Final extension	72	10	1
Hold	4	Indefinitely	

The amplified DNA was then loaded onto an agarose gel and electrophoresis carried out to determine the size of bands against a DNA ladder.

Cell culture medium

Most of the experiments were carried out in RPMI 1640 medium (Invitrogen), supplemented with 10% heat-inactivated fetal bovine serum (FBS) (ThermoScientific) and 1% penicillin-streptomycin-glutamine (PSG) (Invitrogen).

Tissue preparation

Spleens were crushed through a 70µm strainer and resuspended in RPMI medium, supplemented with 10% FBS and 1% PSG. Spleens were then centrifuged at 1500rpm for 5 minutes. The resulting pellet was treated with RBC lysis buffer (Sigma), washed with PBS and resuspended in medium. Perfused liver was minced, pressed through a 100-µm strainer and resuspended in RPMI 1640. Liver cells were spun and the pellet was resuspended in 38% Percoll (GE Healthcare) and then centrifuged at 500g for 20 min at room temperature. Cell pellets were treated with RBC lysis buffer, washed, and resuspended in medium.

iNKT$^+$ selection using CD1d selection

The process of antibody labelled cell selection and QuadroMACS selection took place in several stages. First, splenocytes were surface stained with CD1d-PE (1µl of CD1d was added per $5x10^6$ cells), and incubated at 4ºC for 25 minutes. The cells were washed and subsequently the pellet was incubated with anti-PE beads (20µl per 10^7 cells), resuspended in 500µl of magnetic cell sorting (MACS) buffer (PBS with 2mM EDTA and 0.5% BSA) (Miltenyi Biotec, Surrey, United Kindom) for 15 minutes in the dark at 4ºC. Excessive beads were washed off with 10ml of cold PBS, and the pellet was resuspended in 1ml of MACS buffer. Cell suspensions were run through a LS column (Miltenyi Biotec, Surrey, United Kingdom) placed in a magnetic field provided by the QuadroMACS. Cells labelled by magnetic beads remained in the column and the depleted fraction went into a collecting tube via flow-through solution. The LS column was then taken away from the magnetic field, washed twice with MACS buffer and iNKT cells were collected in the flow-through through positive selection, iNKT cell purity was > 95%.

Surface staining

For surface staining, cells were washed twice with 1% FBS/PBS and spun. Cells were incubated for 20 minutes at 4ºC with surface antibodies as stated in Table 1. Cells were then washed with 1% FBS/PBS and analyzed on Cyan ADP and further analyzed using FlowJo software (TreeStar, Inc).

Intracellular cytokine staining (ICC)

Previous to the intracellular cytokine staining stage, any surface staining was to be done was carried out before the fixing stage. Cells were then washed with PBS and subsequently fixed with fixation solution fix buffer (BD biosciences) for 20 minutes at 4ºC. Following that, cells were washed twice with 10x PERM buffer (BD biosciences) that allows for permeabilization of cells. This was followed by labelling with specific intracellular cytokine antibodies for 30 minutes at 4ºC (Table 2). A mastermix of antibodies was prepared in 1x PERM buffer, whenever there were several conditions to be stained with a similar antibody cocktail. Cells were washed with 1% FBS/PBS and resuspended in a small volume of PBS. Cells were analyzed on Cyan ADP and further analyzed using FlowJo software (TreeStar, Inc).

Table 2. Antibodies used for surface and intracellular staining.

	Antibody and tetramer (Clone number)	Company
Surface staining	PBS-57 loaded CD1d tetramer	National Institutes of Health Tetramer Facility
	APC-TCRβ (H57-597)	eBiosciences
	FITC-CD3 (145-2C11)	eBiosciences
	FITC-NK1.1 (PK136)	eBiosciences
	FITC-CD8 (53-6.7)	eBiosciences
	PE-Cy7-CD4 (GK1.5)	eBiosciences
	Cxcr2-PE (LMD0410091)	R&D Systems
	eFluor660-GL7 (E15639-103)	eBiosciences
	PE-B220 (E01246-1632)	eBiosciences
	Anti-IL-4 (XMG1.2)	eBiosciences
	Anti-IFN-γ (11B11)	eBiosciences
ICC	RORC-PE (E02046-1630)	eBiosciences
	Phospho p38 MAPK	Cell signaling
	Phospho STAT3	Cell signaling
	Phospho JNK	Cell signaling
	IL-1β-FITC (E13678-102)	eBiosciences
	IL-17-APC (51-7177-80)	eBiosciences
	P27 (JZA0211031)	R&D Systems

Flow cytometry

Flow cytometry was carried out on a Cyan ADP. The original gating was carried out looking at the forward and side scatter to get an idea of the size and the granulosity of the cells in order to pinpoint the lymphocyte population and to exclude dead cells. Voltage parameters were adjusted for that particular gating, subsequently we looked at specific lymphocyte populations such as iNKT, T cells and B cells by recognizing their respective markers for example CD1d for iNKT cells, CD4 for T cells and CD19 for B cells. From those distinct populations more surface and intracellular markers were gated on as listed from table 2.

BrdU labelling

For bromodeoxyuridine (BrdU) labelling, mice were fed with BrdU (0.8 mg/ml) in drinking water supplemented with 5% (weight/volume) glucose one day prior to α-GalCer (2μg) i.p. injection. Mice were treated with BrdU in drinking water for 3 days to study homeostatic proliferation. An equivalent starting number of cells were used in the case of *Map3k1*$^{\Delta KD}$ and *Map3k1*$^{+/\Delta KD}$ mice. They were surface stained and BrdU staining was performed according to the manufacturer's protocol (BD Pharmingen BrdU Flow Kit). Cells were analyzed in a Cyan ADP (DakoCytomation) flow cytometer and further analyzed using FlowJo software (TreeStar).

Enzyme-linked immune absorbent assay (ELISA)

Blood was obtained from mice by cardiac puncture and was stored overnight at 4ºC. It was spun at 5000g for 5 minutes and the serum was collected for ELISA. Samples were measured in triplicates on a 96 well plate. The 96 well plates were coated overnight at 4ºC with 100μl/well of the capture antibody (working concentration for IL-1β 1μg/ml) diluted in PBS. The next day the cells were washed three times with 0.05% Tween-20/PBS using the ELISA plate washer and blocked with 300μl/well of assay diluent (10% FBS/PBS) for one hour at room temperature. The plates were washed three times before plating out the samples and standards. The maximum standard limit for IL-1β was 2000pg/ml. The standards were prepared in assay diluent, as the samples had been in. The standards were plated out in duplicates 100μl/well, starting with the maximum concentration at the

top and diluting by a factor of 1:2 for 7 serial dilutions to reach a final concentration of zero. Samples were plated out 50µl/well in triplicates. After two hours incubation at room temperature, the plates were washed as previously described above and incubated with 100µl/well of detection antibody (1:500 dilution in assay diluents) diluted in assay diluent for 1 hour. The cells were washed and incubated with 100µl/ml of streptavidin horseradish enzyme reagent diluted 1:250 in assay diluent for 30 minutes at room temperature . Plates were then washed six times and 100µl/well of substrate solution tetramethylbenzemidine (TMB) (Invitrogen) was added and incubated until the standard had fully developed observed from the colour change into an appropriate blue colour. Following that, 50µl of stop solution (2N H_2SO_4) was added with gentle tapping of the plate. The optical density of each well was measure at a wavelength of 450nm using an ELISA reader. The data was analysed using Excel.

RNA isolation

iNKT cell RNA was prepared using RNeasy Kit (Qiagen). The cells were washed in PBS and spun. 350µl of RLT buffer was added for < $5x10^6$ cells. The lysate was transferred into a QIAshredder spin column placed in a 2ml collection tube and spun for 2 minutes at full speed. 70% ethanol was added to the homogenized lysate and the sample transferred to an RNeasy spin column placed in a 2ml collection tube and centrifuged for 15 seconds at 8000xg. The flow through was discarded. The spin column was washed successively. The RNeasy spin column was placed in a new 1.5ml collection tube and 50µl of RNase-free water was added to the spin column membrane and spun for 1 minute at 8000xg to elute the RNA. The RNA pellet was left to air dry and then dissolved in 30-50µl of nuclease free water (Bio-Rad, USA). The concentration of RNA and its quality was evaluated using spectrum NanoDrop (ThermoScientific, USA). A ratio of absorbance at 260nm/280nm of about 2.0 is generally accepted as pure for RNA. The samples were stored at -80ºC.

Conversion of mRNA

cDNA was transcribed using cDNA RT-Kit (Applied Biosystems). Following the manufacturers protocol, each 20µl reaction mixture contained the 10µl RNA templates (500µg mRNA), 2µl 10x RT

buffer, 0.8µl 25x dNTP mix, 2µl 10x random primers, 1µl reverse transcriptase, 1µl RNase inhibitor and 3.2µl nuclease free water. The PCR (Veriti Thermal Cycler, Applied biosystems) amplification programme was set to the following: 25ºC for 10 minutes, 37ºC for 120 minutes, 85ºC for 5 minutes and a final temperature at 4ºC. cDNA was stored at -20ºC for future use.

Quantitative Reverse transcription polymearase chain reaction (qRT-PCR)

qRT-PCR primers (Table 3) were purchased from Invitrogen. SyBr Green (Applied biosystems) was used as a reporter. Experiments were performed using the 384-well reaction plate (ABgene, USA). Each reaction contained gene-specific testing primers and SyBr green reporter namely IL-17A and RORC. β-actin was used as a housekeeping gene. Multiplex experiments were done in triplicates, with each well containing 20µl of reaction mix comprising of 5µl template cDNA, 0.3µl testing primer, 10µl SyBr green and 4.4µl nuclease free water. The reaction plate was briefly spun to limit the number of bubbles. The plate was loaded onto the ABI prism 7900 HT Sequence Detection System (Applied Biosystems, Cheshire, UK) and the plate was run from the SDS2.1 software (Applied Biosystems). The thermal cycling profile was as follows 50ºC for 2 minutes, 95ºC for 15 minutes, then 45 cycles of amplification at 94ºC for 15 seconds and 59ºC for 30 seconds and 72ºC for 30 seconds. The comparative method for quantification was used for analysis, since quality control and amplification efficiencies of the genes were equivalent Threshold Cycle (Ct) values generated were exported from the SDS2.1 software to Microsoft Excel for further analysis.

Interpretation of qRT-PCR data

This was a relative quantification method which did not provide information of absolute copy number of mRNA. Instead, it estimated the increase or decrease in target mRNA compared with β-actin (internal control). The main indicator used here was the Threshold Cycle (Ct) value, which was recorded by the device when the detecting fluorescence increased beyond an arbitrary cut off point. In theory, more starting material correlated with higher fluorescence hence lower Ct values. The different Ct values between internal and stimulation controls (ΔCt) was used to evaluate the relative mRNA expression level.

qRT-PCR was performed as described above. For every sample, there were Ct values for specific gene of interest (Ct_{gene}) or β-actin (Ct_{beta}); and the ΔCt for each culture conditions followed the algorithm as the following:

$$\Delta Ct_{reaction} = (Ct_{gene} - Ct_{beta})_{reaction}$$

Mean values were calculated for the triplicate samples. Since the ΔCt value inversely correlated with the abundance of starting material, in practice, the $-\Delta Ct_{reaction}$ was more commonly used so that a positive value related with increased mRNA level during certain stimulation and vice versa.

$$\text{Relative Quantification} = 2^{-\Delta Ct}$$

Table 3. Primer sequences used for real-time PCR.

	5' to 3'	
	Forward Primer	Reverse Primer
β-actin	GTCGACAACGGCTCCGGCATGT	TCCCACCATCACACCCTGGTGCCTA
Ar	TGAGCCAGGAGTGGTGTGTGC	AAGTTGCGGAAGCCAGGCAAGG
Camp	AGGAACAGGGGGTGGTGAAGCA	AGAAGTCCAGCCAGCCGGGAA
Cdkn1b	GCCAGACGTAAACAGCTCCGAATTA	AGAGGCAGATGGTTTAAGAGTGCCT
CD101	AGTTTCTGCTAAGTTCAGCATCGGC	TTCCTTGGTCGGGGCGCTTG
CD177	CCTTGCTACCCTGTGTCCCAGC	GGCAACCCTCGCTAACCTCGC
CD33	GGGGAGGCAACGGTCAAGCTC	CCTGCTGATGAGCCTGTGTATGGAA
Clec4d	ACCCGACATCCCCAACTGATCCC	GCAGGTCCAAGTACCTCCTGTAGC
Csf3r	ACCCCATGGATGTTGCCCCC	CTTCCTGCAGGGGCGTTGGC
Cxcr2	ATCTTCGCTGTCGTCCTTGT	AGCCAAGAATCTCCGTAGCA
Il17rb	GGAGGCAAGGAAGGAGCACGA	CGGCCCCATCTCGGCGATTT
Il1b	CCCTGCAGCTGGAGAGTGTGGA	TGTGCTCTGCTTGTGAGGTGCTG
Il1f9	CCACAGAGTAACCCCAGTCAGCG	TTCCACCTGTCCGGGTGTGGT
Il1r2	CGGGTCAAAGGAACAACCACGGA	CGGTCACACGGCCTCTTGGG
klk1b11	CACCCACGAAATTCCAAACCCCAG	CCGGCGTATTGGGTTTGCCACA
klrc3	AGACAGTGAAGAGGAGCAGGACTTT	TCTGCTGTGAGACCAGAAGCTGAC
klrk1	TCTGCTCAGAGATGAGCAAATGCC	GCCAAGGCTATAGCAAGGACTCGAA
Mmp9	TGCCCTACCCGAGTGGACGC	AGCCCAGTGCATGGCCGAAC
Ppbp	TCCTTGTTGCGCTGGCTCCC	GTGTGGCTATCACTTCCACATCAGC
Ptger1	ACATGCATGGGGTGGAGCAGC	TATCAGTGGCCAAGAGGGCCAG
Retnla	CCTGCCCTGCTGGGATGACT	GGGCAGTGGTCCAGTCAACGA
Rorc	TTCCCACTTCCTCAGCGCCC	TGGGTGGCAGCTTGGCTAGGA
Tdgf1	TCGCAAAGAGCACTGTGGGTC	AGTGGTCGTCACAGACGGCG

Peripheral blood isolation

The research group took peripheral blood from mice was obtained by cardiac puncture. One part blood was layered onto one part lymphocyte separation media Ficoll-Paque (GE Healthcare) and centrifuged for 15 minutes at 700g. PBMCs were collected from the interface layer and washed with sterile PBS.

Microarray and bioinformatics analysis

For microarray and bioinformatics analysis the research group took total RNA from iNKT cells and reverse transcribed it into biotinylated cRNA with an RNA Amplification kit as stated in the manufacturer's directions (Ambion). Quality of RNA was confirmed using a 2100 Bioanalyzer (Agilent Technologies). Samples were hybridized to Mouse Gene 1.0 ST arrays (Affymetrix). Partek software was used (as stated in vendor protocols) for data analysis, quality control, and for creating gene lists and scatter plots. GeneSpringX software was used (as stated in vendor protocols) to produce heat maps. Probes with a fold change less than 2 were discarded and a list of relevant gene targets were selected (Table 3). Probes were quantile normalized among all microarray data. Gene lists were uploaded into the IPA program (Ingenuity Systems) to generate relevant signaling networks (according to the vendor instructions).

Table 3: Global changes in gene expression between *Map3k1*$^{+/\Delta KD}$ and *Map3k1*$^{\Delta KD}$ iNKT cells.

ID	Fold Change	Entrez Gene Name	Location	Type(s)
Klrc3	2.799	killer cell lectin-like receptor subfamily C, member 2	Plasma Membrane	other
Ar	2.397	androgen receptor	Nucleus	ligand-dependent nuclear receptor
Klrk1	2.266	killer cell lectin-like receptor subfamily K, member 1	Plasma Membrane	transmembrane receptor
Klk1b11	2.186	kallikrein-related peptidase 3	Extracellular Space	peptidase
Cd101	-2.008	CD101 molecule	Plasma Membrane	other
Cd177	-2.039	CD177 molecule	Cytoplasm	other
Clec4d	-2.042	C-type lectin domain family 4, member D	Plasma Membrane	other
Il1r2	-2.054	interleukin 1 receptor, type II	Plasma Membrane	transmembrane receptor
Rorc	-2.066	RAR-related orphan receptor C	Nucleus	ligand-dependent nuclear receptor
Cd33	-2.078	CD33 antigen	Plasma Membrane	other
Tdgf1	-2.110	teratocarcinoma-derived growth factor 1	Extracellular Space	growth factor
Il1b	-2.152	interleukin 1, beta	Extracellular Space	cytokine
Camp	-2.230	cathelicidin antimicrobial peptide	Cytoplasm	other
Csf3r	-2.246	colony stimulating factor 3 receptor (granulocyte)	Plasma Membrane	transmembrane receptor
Cxcr2	-2.257	chemokine (C-X-C motif) receptor 2	Plasma Membrane	G-protein coupled receptor
Il17rb	-2.345	interleukin 17 receptor B	Plasma Membrane	transmembrane receptor
Mmp9	-2.345	matrix metallopeptidase 9 (gelatinase B, 92kDa gelatinase, 92kDa type IV collagenase)	Extracellular Space	peptidase
Cdkn1b	-2.386	cyclin-dependent kinase inhibitor 1B (p27, Kip1)	Nucleus	kinase
Retnla	-2.628	resistin like alpha	Extracellular Space	other
Rbm39	-2.672	RNA binding motif protein 39	Nucleus	transcription regulator
Il1f9	-2.699	interleukin 36, gamma	Extracellular Space	cytokine
Rapgef1	-2.914	Rap guanine nucleotide exchange factor (GEF) 1	Cytoplasm	other
Ptger1	-3.025	prostaglandin E receptor 1 (subtype EP1), 42kDa	Plasma Membrane	G-protein coupled receptor

Liver damage assay

The research group injected mice i.v. with 5µg KRN7000. After 3 days, the livers were harvested, fixed in 4% paraformaldehyde, processed and paraffin-embedded. H&E staining was carried out on liver sections. Slides were analyzed using an Olympus light microscope (original magnification x20) and pictures were taken using Image Pro-Software.

Statistical analysis

Data is expressed as SEM. Statistical significance was determined by two-tailed Student's t-test. All analyses were performed using GraphPad Prism 5 software (GraphPad) and Microsoft Excel.

Results

Disruption of *Map3k1* and *Map3k7* does not alter iNKT cell development

To examine the role of *Map3k1* and *Map3k7* in iNKT development, flow cytometry analysis of the spleen, thymus, bone marrow and liver from *Map3k1*$^{\Delta KD}$, *Lck-Cre*$^{+}$*Map3k7*$^{f/f}$ and control mice was performed. There was no difference observed between the number of iNKT CD1d^{+}CD3^{+} cells and no significant developmental defect in these organs between *Map3k1*$^{\Delta KD}$, *Lck-Cre*$^{+}$*Map3k7*$^{f/f}$ and control mice (Fig. 6).

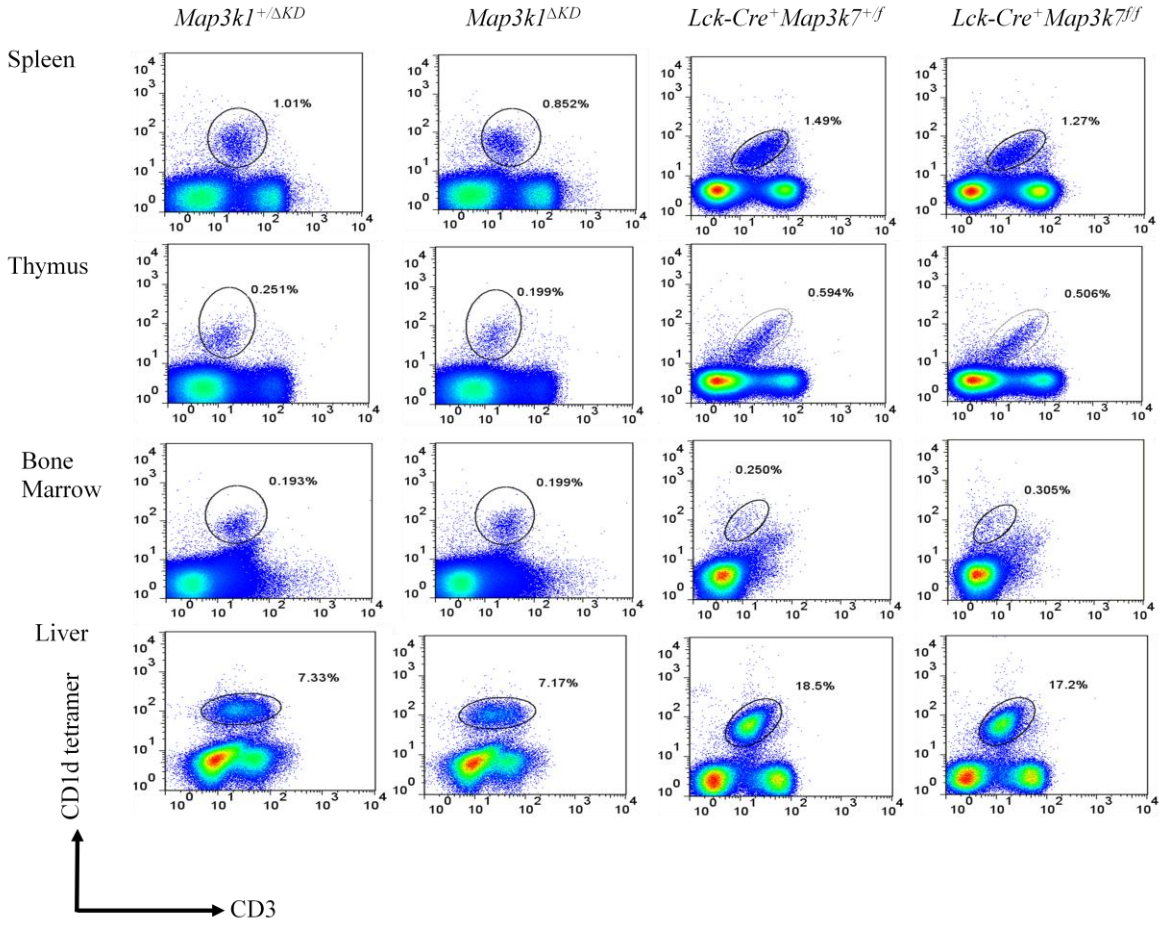

Fig 6. iNKT cell development in *Map3k1*$^{\Delta KD}$ and *Lck-Cre*$^{+}$*Map3k7*$^{f/f}$ mice.
Splenocytes, thymocytes, bone marrow and liver cells from *Map3k1*$^{\Delta KD}$, *Map3k1*$^{+/\Delta KD}$, *Lck-Cre*$^{+}$*Map3k7*$^{f/f}$ and *Lck-CreMap3k7*$^{+/f}$ mice were isolated and stained with CD1d tetramer and anti-CD3 antibody and analyzed using flow cytometry as stated in the materials and methods. No observed difference was seen between the numbers of iNKT CD1d^{+}CD3^{+} cells in *Map3k1*$^{\Delta KD}$, *Lck-Cre*$^{+}$*Map3k7*$^{f/f}$ and control mice. Data was representative of 3 mice per group from 3 independent experiments.

The profiles of $CD4^+$ and $CD8^+$ T cell subsets were analyzed in *Map3k1*$^{\Delta KD}$, *Lck-Cre*$^+$*Map3k7*$^{f/f}$ and no significant difference was found in comparison with control mice, revealing that normal lymphocyte development is able to occur in the absence of *Map3k1* and *Map3k7* without antigen stimulation (Fig. 7).

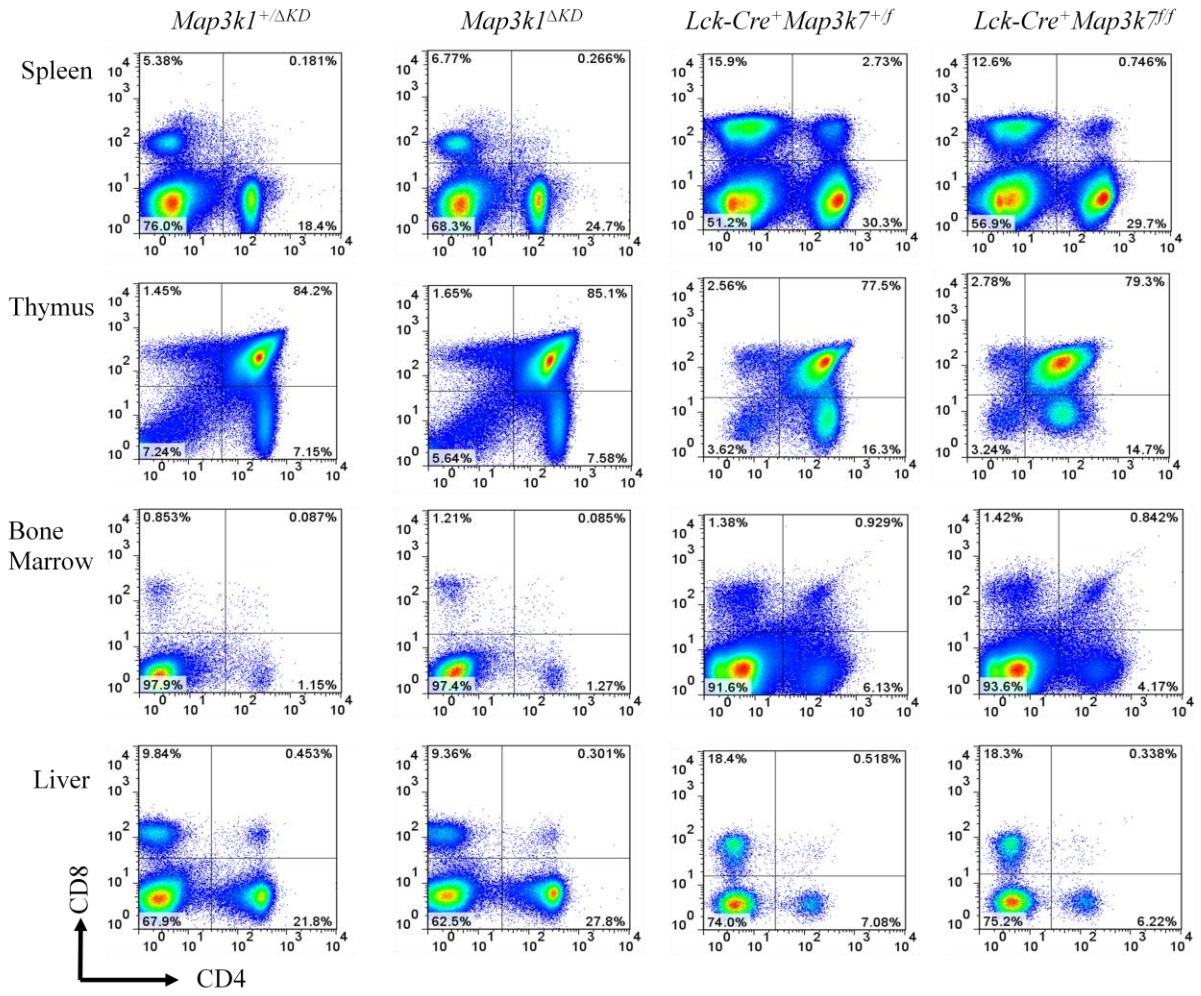

Fig 7. iNKT development in *Map3k1*$^{\Delta KD}$ and *Lck-Cre*$^+$*Map3k7*$^{f/f}$ mice.
Splenocytes, thymocytes, bone marrow and liver cells from *Map3k1*$^{+/\Delta KD}$, *Lck-Cre*$^+$*Map3k7*$^{f/f}$ and *Lck-CreMap3k7*$^{+/f}$ mice were isolated and stained with anti-CD4 and anti-CD8 antibodies and analyzed by flow cytometry. No significant difference in lymphocyte development was found in *Map3k1*$^{\Delta KD}$, and *Lck-Cre*$^+$*Map3k7*$^{f/f}$ compared with control mice. Data was representative of 3 mice per group from 2 independent experiments.

Map3k1 and *Map3k7* kinases differently regulate the splenic iNKT clonal burst

To establish whether there is a role for *Map3k1* kinase signaling in effector iNKT cell responses to glycolipid antigens, splenic iNKT cells were stimulated via i.p. injection of the α-GalCer analog KRN7000 into *Map3k1*$^{\Delta KD}$ and control mice over a period of 6 days to lead to an expansion of splenic iNKT cells. A peak response of iNKT cells was observed on day 3 followed by a steep decline on day 6 to numbers of an unstimulated level (Fig. 8). Reduced numbers of iNKT cells in *Map3k1*$^{\Delta KD}$ mice on day 3 suggest a defect in iNKT expansion.

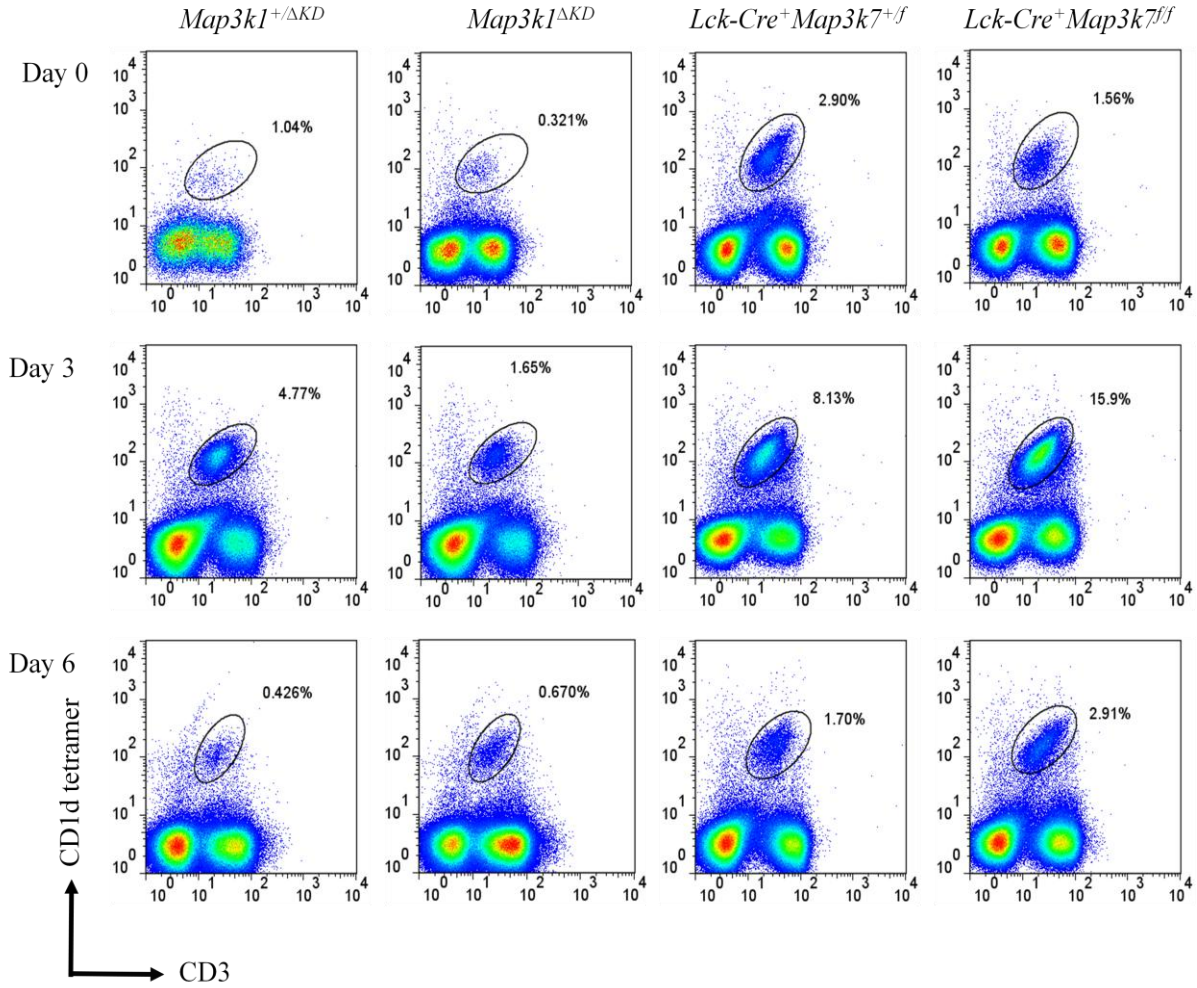

Fig 8. iNKT cell expansion in *Map3k1*$^{\Delta KD}$, *Map3k1*$^{+/\Delta KD}$, *Lck-Cre*$^{+}$*Map3k7*$^{f/f}$ and *Lck-CreMap3k7*$^{+/f}$ mice.
i.p. injections of α-GalCer were administered to *Map3k1*$^{\Delta KD}$, *Map3k1*$^{+/\Delta KD}$, *Lck-Cre*$^{+}$*Map3k7*$^{f/f}$ and *Lck-CreMap3k7*$^{+/f}$ mice over a 6 day time period. Splenocytes were harvested at days 0, 3 and 6, stained with CD1d tetramer and anti-CD3 antibody and analyzed using flow cytometery. A peak response of iNKT cells was observed on day 3 followed by a steep decline on day 6 to numbers corresponding to an unstimulated level. Data was representative of 3 mice per group from 3 independent experiments.

Molecular basis of the defective *Map3k1$^{\Delta KD}$* iNKT clonal burst

As it was observed that there was an iNKT cell expansion defect in *Map3k1$^{\Delta KD}$* mice and enhanced iNKT expansion in *Lck-Cre^{+}Map3k7$^{f/f}$* mice upon antigenic stimulation (Fig. 8 and 9A), we wanted to assess the molecular mechanisms during this effect. Day 3 isolated iNKT cell mRNA from *Map3k1$^{+/\Delta KD}$* and *Map3k1$^{\Delta KD}$* mice was processed and hybridized onto Affymetrix Mouse Gene 1.0 ST arrays to compare the gene expression profiles between the two groups. Affymetrix array profiling revealed changes in gene expression between *Map3k1$^{+/\Delta KD}$* and *Map3k1$^{\Delta KD}$* iNKT cells at day 3. Significant microarray hits with a gene expression change of higher than 2 fold between the two genetic groups were identified; several are involved in inflammation and immune responses (*Cxcr2, CD101, Il1f9, Il1r2, Il1β, Rorc, Il17rb and Mmp9*) and cell proliferation (*Cdkn1b*) (Fig. 9B and C). Presence of the metalloproteinase *Mmp9*, the transcription factor *Rorc/Rorγt (Ivanov et al., 2006)*, and the IL-17 receptor family *Il17rb*, suggested that IL-17 and Th17 cell signaling pathways support the iNKT cell clonal burst defect found in *Map3k1$^{\Delta D}$* mice (Gaffen, 2009). Microarray screened IL1β and IL1β-related genes (*Il1f9* and *Il1r2*) show an association between *Map3k*-dependent iNKT gene expression and the p38 signaling pathway (Arana-Argaez et al., 2010; Inoue et al., 2006). JNK and p38 MAPK activation was reduced in *Map3k1$^{\Delta KD}$* iNKT cells at day 3 relative to control (Fig. 9D).

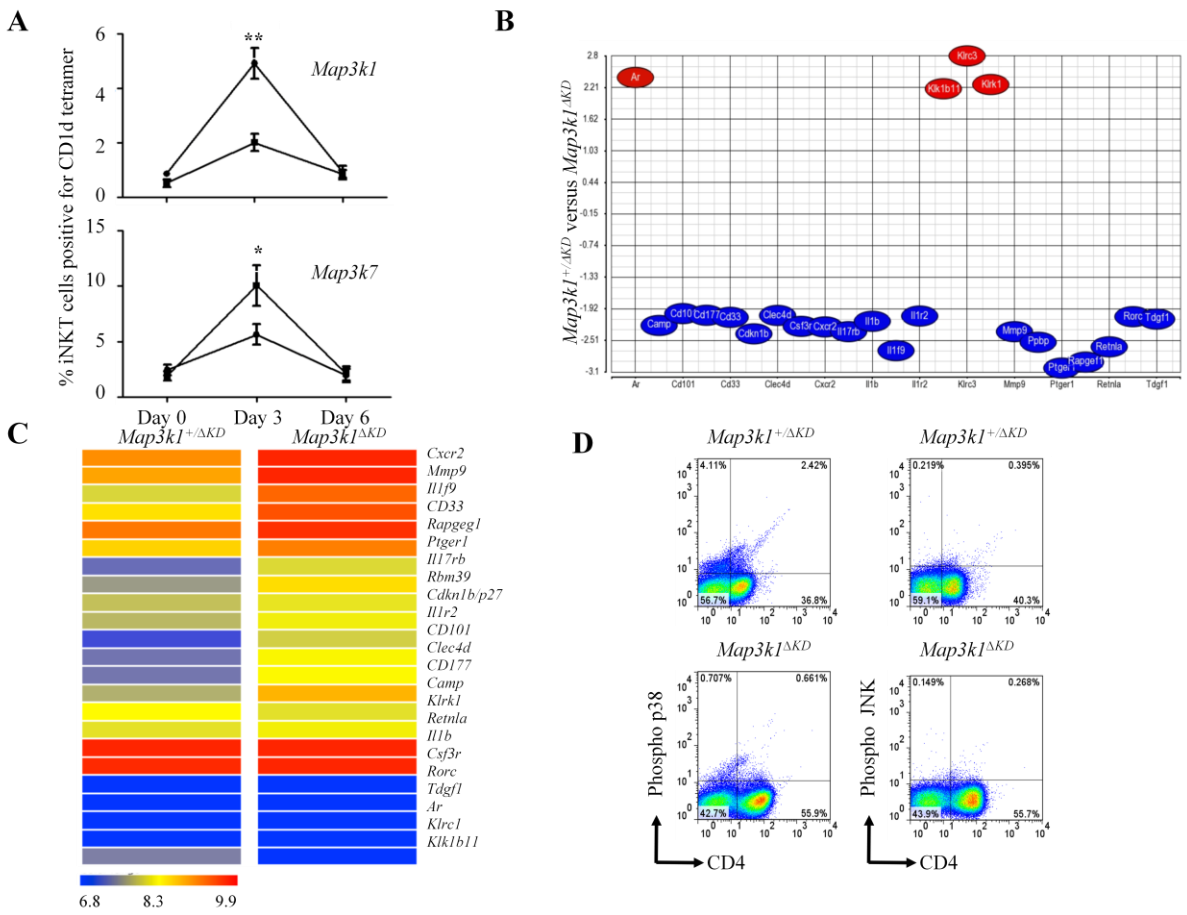

Fig 9. Microarray and bioinformatics analysis of the *Map3k*-dependent iNKT cell expansion defect.

Map3k1$^{+/\Delta KD}$, *Map3k1*$^{\Delta KD}$, *Lck-Cre*$^{+}$*Map3k7*$^{+/f}$ and *Lck-Cre*$^{+}$*Map3k7*$^{f/f}$ mice were injected i.p. with α-GalCer to stimulate iNKT cells over a 6 day period. Splenocytes were harvested at days 0, 3 and 6, processed and stained with a CD1d tetramer, anti-CD3 and anti-TCRβ antibodies and analyzed by flow cytometry as stated in the materials and methods. (A) Statistical analysis of iNKT expansion at days 0, 3 and 6. The average percentage (± SEM) of CD1d^{+} cells from 5 independent experiments is shown (3 mice per experiment). The upper panel corresponds to the *Map3k1* genotype (•*Map3k1*$^{+/\Delta KD}$ and ■ *Map3k1*$^{\Delta KD}$) and the lower panel corresponds to the *Map3k7* genotype (•*Lck-Cre*$^{+}$*Map3k7*$^{+/f}$ and ■ *Lck-Cre*$^{+}$*Map3k7*$^{f/f}$). Differences were analyzed by two-tailed students t-test (*, $p \leq 0.05$; **, $p \leq 0.01$). A peak response of iNKT cells was observed on day 3 followed by a steep decline on day 6 to numbers of an unstimulated level. (B) RNA was isolated from *Map3k1*$^{+/\Delta KD}$ and *Map3k1*$^{\Delta KD}$ iNKT cells, processed and hybridized onto Affymetrix arrays as stated in the materials and methods. Bioinformatics analysis was performed as stated in the materials and methods. Microarray screened genes with a greater than 2-fold difference between the *Map3k1*$^{+/\Delta KD}$ and *Map3k1*$^{\Delta KD}$ groups was shown in a scatter plot. A few genes involved in immune responses and apoptosis showed differential expression between the experimental and control mice. (C) A heat map comparing gene hits with a greater than 2-fold difference between *Map3k1*$^{+/\Delta KD}$ and *Map3k1*$^{\Delta KD}$ groups was generated. *Map3k1*$^{+/\Delta KD}$ and *Map3k1*$^{\Delta KD}$ iNKT microarray screens were constructed as described in the material and methods. Colour intensity indicates the range of upregulation (9.9) versus downregulation (6.8) across genes compared between the *Map3k1*$^{+/\Delta KD}$ and *Map3k1*$^{\Delta KD}$ groups. (D) iNKT splenic cells were isolated from 3-day α-GalCer stimulated *Map3k1*$^{\Delta KD}$ and control mice, as stated in the materials and methods, and were stained with CD1d tetramer, anti-CD4, anti-phospho-JNK, and anti-phospho-p38 antibodies, and analyzed by flow cytometry. It can be seen that JNK and p38 MAPK activation was reduced in *Map3k1*$^{\Delta KD}$ iNKT cells at day 3 relative to control.

Map3k1$^{\Delta KD}$ iNKT cells hypoproliferate during their clonal burst

The reduced expression of the *Map3k1*$^{\Delta KD}$ iNKT cell splenic population, and enhanced *Cdkn1b* gene overexpression in *Map3k1*$^{\Delta KD}$ mice propose that p27 (encoded by *Cdkn1b*) expression is a *Map3k*-dependent molecular mechanism that regulates iNKT cell proliferation, as p27 is a cell cycle inhibitor which binds to and prevents the activation of cyclin E-CDK2 or cyclin D-CDK4 complexes and negatively regulates cell cycle progression at G1 (Kiyokawa et al., 1996). iNKT cell proliferation in *Map3k1*$^{\Delta KD}$ mice was examined next. *Map3k1*$^{\Delta KD}$ and *Map3k1*$^{+/\Delta KD}$ mice were treated with BrdU and then immunized by i.p. injection of α-GalCer. Splenocytes were extracted and equal numbers of cells from both groups were analyzed by FACS at day 3 post immunization for BrdU incorporation. iNKT cells extracted from *Map3k1*$^{\Delta KD}$ mice hyporoliferated relative to control mice (Fig. 10A), and *Map3k1*$^{\Delta KD}$ iNKT cells incorporated approximately half the BrdU of control iNKT cells (Fig. 10B). The upregulation of p27 expression in *Map3k1*$^{\Delta KD}$ mice was confirmed by microarray gene screening at the mRNA level by an orthogonal real-time PCR approach (Fig. 10C, left panel) at the level of protein expression by Western blotting (Fig. 10D) and at the cellular level by flow cytometry (Fig. 10E). By contrast, p27 expression was reduced in *Lck-Cre*$^{+}$*Map3k7*$^{f/f}$ mice, which explains the enhanced iNKT expansion seen in *Lck-Cre*$^{+}$*Map3k7*$^{f/f}$ mice (Fig. 10C, middle panel).

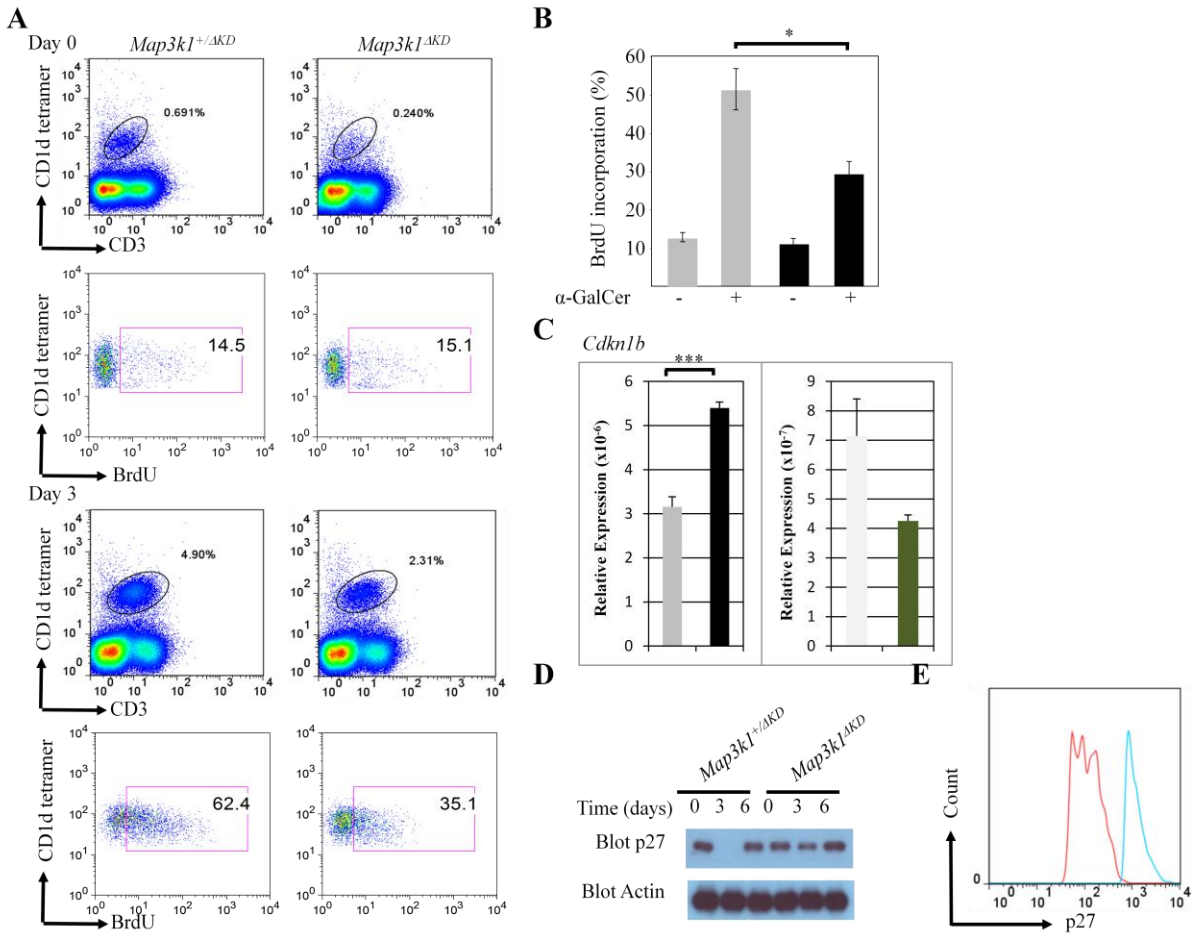

Fig 10. Hypoproliferation of iNKT cells in *Map3k1$^{\Delta KD}$* mice.
(A) *Map3k1$^{\Delta KD}$* and *Map3k1$^{+/\Delta KD}$* mice were treated with water containing BrdU, i.p. immunized with α- GalCer (Day 3) or left unimmunized (Day 0). Splenocytes from *Map3k1$^{+/\Delta KD}$* (left panels) and *Map3k1$^{\Delta KD}$* (right panels) were stained with CD1d tetramer, anti-BrdU and anti-CD3 antibodies. It can be seen that iNKT cells extracted from *Map3k1$^{\Delta KD}$* mice hyporoliferated relative to control mice. (B) Representative results from 3 quantitated iNKT proliferation experiments were statistically analysed, where appropriate, by two-tailed Student's t test (*, $p \leq 0.05$) (■*Map3k1$^{+/\Delta KD}$* and ■*Map3k1$^{\Delta KD}$*). It was observed that *Map3k1$^{\Delta KD}$* iNKT cells incorporated approximately half the BrdU of control iNKT cells. (C) RNA was extracted from isolated iNKT cells (■*Map3k1$^{+/\Delta KD}$*, ■*Map3k1$^{\Delta KD}$*, ■*Lck-Cre^{+}Map3k7$^{+/f}$*, ■*Lck-Cre^{+}Map3k7$^{f/f}$*), reverse transcribed, and real-time PCR performed as stated in the materials and methods. The average relative expression (± SEM) of *Cdkn1b* (*p27*) mRNA from 3 independent experiments was statistically analysed, where appropriate, by two-tailed Student's t test (***, $p \leq 0.001$). It was observed that there was an upregulation of *p27* expression in *Map3k1$^{\Delta KD}$* mice (left panel) while *p27* expression was reduced in *Lck-Cre^{+}Map3k7$^{f/f}$* mice (right panel). (D) Western blot analysis of *p27* expression in isolated iNKT cells from *Map3k1$^{+/\Delta KD}$* and *Map3k1$^{\Delta KD}$* mice at 0, 3 and 6 days post i.p. injection with α-GalCer. Higher protein expression of *p27*in *Map3k1$^{\Delta KD}$* at day 3 was observed. (e) iNKT cells from *Map3k1$^{\Delta KD}$* and control mice were stained with anti-p27 antibody and FACS performed (- *Map3k1$^{+/\Delta KD}$*, and - *Map3k1$^{\Delta KD}$*). Higher percentage of *p27* positive cells were observed in *Map3k1$^{\Delta KD}$* compared to control mice.

IL-17 and *Th17* cell signaling pathways play a role in an underlying defect in *Map3k1*$^{\Delta KD}$ iNKT cells

As a subset of microarray hits were related to the IL-17 and Th17 differentiation pathways, their expression was confirmed using orthogonal approaches. At day 3 of the iNKT clonal burst, phosphorylated STAT3 which is an important transcription factor in the Th17 developmental pathway (Chen et al., 2006), was reduced in *Map3k1*$^{\Delta KD}$ iNKT cells compared to their control by flow cytometry and Western blot assays (Fig.11A and B). *Il17rb* and *Rorc* displayed enhanced expression at the mRNA level, confirming the microarray screening analysis (Fig. 11C). Flow cytometry also confirmed the enhanced expression of *Rorc* in *Map3k1*$^{\Delta KD}$ mice at the cellular level (Fig. 11D). As phosphorylated STAT3 is upstream of *Rorc* in the Th17 signaling pathway (Ivanov et al., 2006), it is notable that the expression of these two transcription factors did not correlate in iNKT cells. *Rorc* is constitutively expressed in human memory Foxp3^{+} regulatory T cells that secrete IL-17 (Ayyoub et al., 2009) and iNKT cells have been described as showing constitutive *Rorc* expression (Rachitskaya et al., 2008). There is no difference between *Il17rb* and *Rorc* expression in *Lck-Cre*$^{+}$*Map3k7*$^{f/f}$ and control iNKT cells (Fig. 11C). Enhanced IL-17 production was seen in *Map3k1*$^{\Delta KD}$ iNKT cells and correlated with upregulated expression of Th17 related genes from the iNKT cell microarray screening (Fig. 11E).

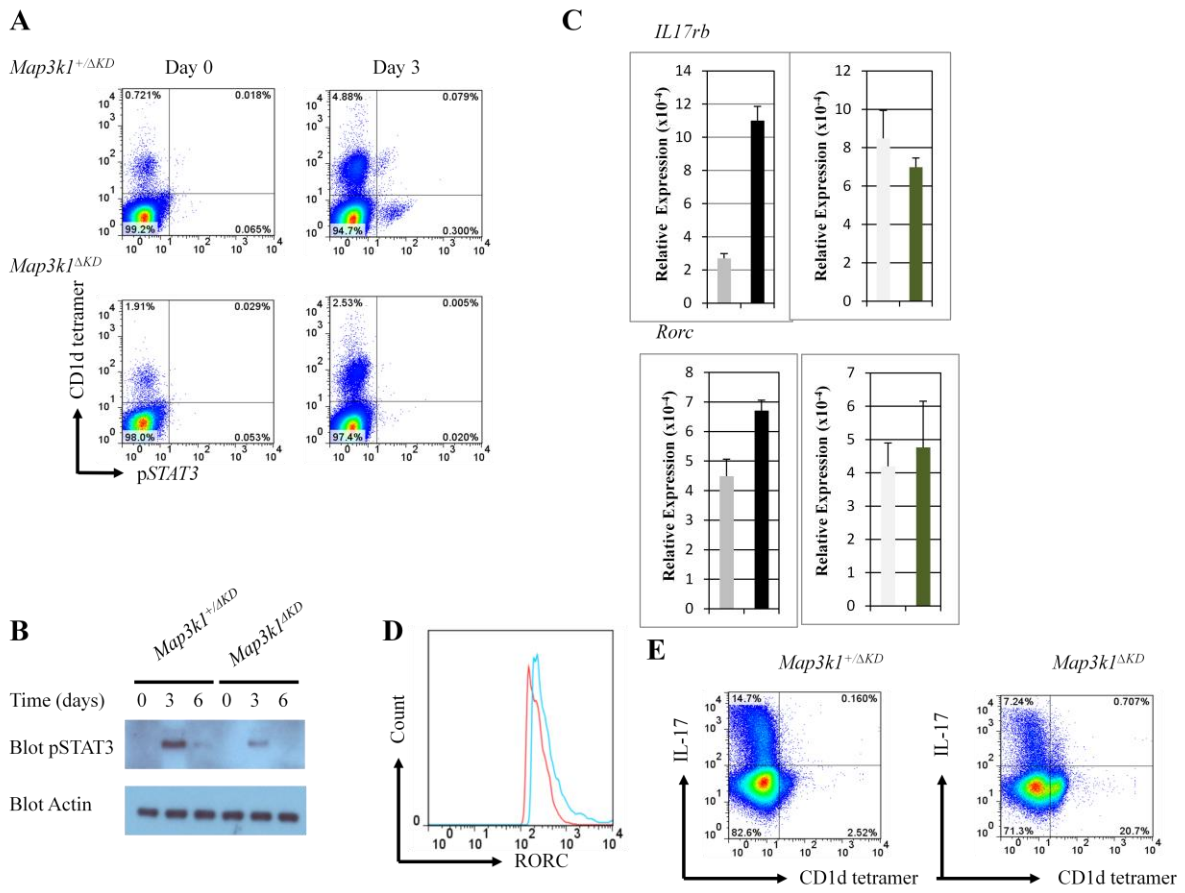

Fig 11. *Map3k*-dependent Th17 and IL-17 signaling pathways regulate iNKT cells.
Splenic iNKT cells were isolated from *Map3k1*$^{\Delta KD}$, *Lck-Cre*$^{+}$*Map3k7*$^{f/f}$, *Lck-Cre*$^{+}$*Map3k2*$^{-/-}$*Map3k3*$^{f/f}$, and control mice following i.p. injection with α-GalCer. (A) iNKT cells from *Map3k1*$^{\Delta KD}$ and control mice were stained with CD1d tetramer and anti-phospho-STAT3 antibody and analyzed by flow cytometry. It was observed that at day 3 phosphorylated *STAT3* was reduced in *Map3k1*$^{\Delta KD}$ iNKT cells compared to their control. (B) Western blot analysis of phospho-STAT3 expression in lysed iNKT cells from *Map3k1*$^{+/\Delta KD}$ and *Map3k1*$^{\Delta KD}$ mice over a 6-day timecourse following i.p. injection with α-GalCer. It was observed that phosphorylated *STAT3* was reduced in *Map3k1*$^{\Delta KD}$ iNKT cells compared to the control cells. (C) RNA was extracted from isolated iNKT cells (■*Map3k1*$^{+/\Delta KD}$, ■*Map3k1*$^{\Delta KD}$, ■*Lck-Cre*$^{+}$*Map3k7*$^{+/f}$, ■*Lck-Cre*$^{+}$*Map3k7*$^{f/f}$mice), reverse transcribed, and real-time PCR was performed. The average relative expression (± SEM) of *Il17rb* and *Rorc* mRNA from 3 independent experiments was statistically analysed, where appropriate, by two-tailed Student's t test (*, $p \leq 0.05$; ***, $p \leq 0.001$). It was seen that there was enhanced expression of *Il17rb* at the mRNA level (D) iNKT cells from *Map3k1*$^{\Delta KD}$ and control mice (- *Map3k1*$^{+/\Delta KD}$, and - *Map3k1*$^{\Delta KD}$) were stained with anti-Rorc antibody and FACS performed. There was enhanced expression of *Rorc* in *Map3k1*$^{\Delta KD}$ mice at the cellular level (E) Stimulated splenocytes were stained with CD1d tetramer, and anti-IL-17 antibodies, and flow cytometry analysis performed. There was enhanced *IL-17* production in *Map3k1*$^{\Delta KD}$ iNKT cells. Data was representative of 3 independent experiments.

Confirmation of other hits generated from *Map3k1*$^{+/\Delta KD}$ and *Map3k1* $^{\Delta KD}$ iNKT cell microarray

Following the findings obtained from the gene expression profile of the iNKT microarray screening, real-time PCR was carried out to further compare gene expression profiles between these two genotypes. It was identified that there was an elevated expression of IL-1β in *Map3k1*$^{\Delta KD}$ iNKT cells and enhanced expression of IL-1β related genes *Il1r2* and *Il1f9* at the molecular level. It was confirmed that there was an upregulation of *Cxcr2*, *CD101*, *CD33*, *CD177* and *Mmp9* genes in *Map3k1*$^{\Delta KD}$ iNKT cells (Fig. 12A). Elevated expression of IL-1β in *Map3k1*$^{\Delta KD}$ iNKT cells was confirmed at the cellular level (Fig 12B). There was also consistently increased secretion of IL-1β in *Map3k1*$^{\Delta KD}$ mice at the protein level, as measured by ELISA from serum of *Map3k1*$^{\Delta KD}$ mice (Fig. 12C). The upregulation of *Cxcr2* gene in *Map3k1*$^{\Delta KD}$ iNKT cells was verified at the cellular level (Fig. 12D).

.

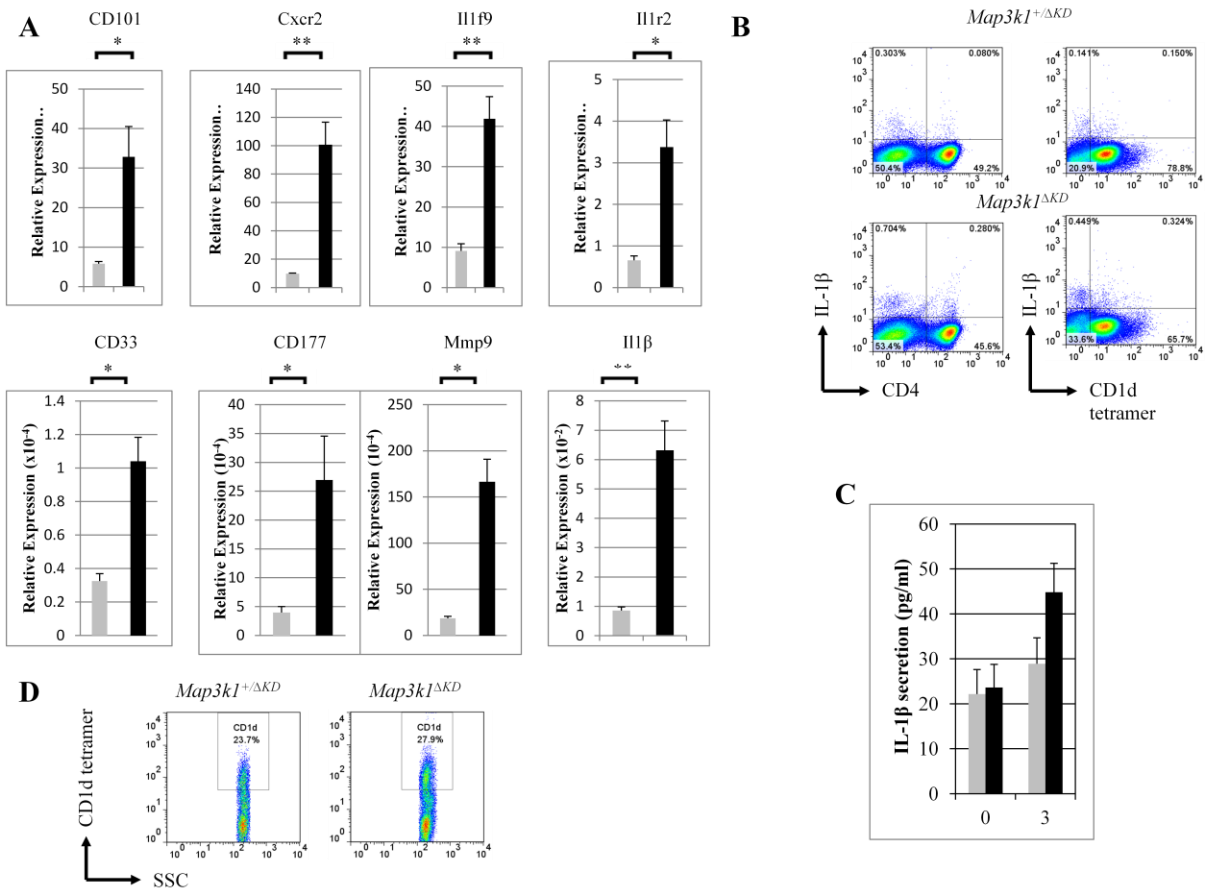

Fig 12. Confirming the expression of microarray hits in *Map3k1$^{\Delta KD}$* iNKT cells
(A) iNKT splenic cells were isolated from *Map3k1$^{\Delta KD}$* and *Map3k1$^{+/\Delta KD}$* mice that had been stimulated with α-GalCer for 3 days. RNA was extracted from iNKT cells (▒ *Map3k1$^{+/\Delta KD}$* and ■ *Map3k1$^{\Delta KD}$*) for *CD101*, *Cxcr2*, *Il1f9*, *Il1r2*, *CD33*, *CD177*, *Mmp9* and *Il1β* and real-time PCR was performed. An upregulation of *Cxcr2*, *CD101*, *CD33*, *CD177* and *Mmp9* genes in *Map3k1$^{\Delta KD}$* iNKT cells was seen. (B) iNKT cells were stained with CD1d tetramer, anti-CD4, and anti-IL-1β antibodies. Flow cytometry analysis was performed. An elevated expression of *IL-1β* in *Map3k1$^{\Delta KD}$* iNKT cells was confirmed at the cellular level. (C) ELISA was carried out on serum obtained from day 3-stimulated mice (▒ *Map3k1$^{+/\Delta KD}$* and ■ *Map3k1$^{\Delta KD}$* mice). IL-1β secretion was evaluated at the protein level. A consistently increased secretion of IL-1β in *Map3k1$^{\Delta KD}$* mice at the protein level wass seen. (D) FACS analysis was performed using anti-Cxcr2 antibody in *Map3k1$^{+/\Delta KD}$* (left panel) and *Map3k1$^{\Delta KD}$* (right panel) iNKT cells. Cxcr2^{+} cells were gated and analysed for CD1d expression. An upregulation of *Cxcr2* gene in *Map3k1$^{\Delta KD}$* iNKT cells was observed.

Role of *Map3k1* in the regulation of iNKT expansion in the liver and peripheral blood mononuclear cells (PBMC), and liver damage in mice

iNKT cell expansion was examined in the liver and PBMC due to the defective iNKT cell splenic expansion seen in *Map3k1*$^{\Delta KD}$ mice (Fig. 13). *Map3k1*$^{\Delta KD}$ mice immunized with α-GalCer led to an expansion of iNKT cells in the liver with a peak response on day 3, followed by a steep decline in the number of iNKT cells to unstimulated levels by day 6 in the liver (Fig.13A). iNKT expansion increased by less than 2 fold in the *Map3k1*$^{\Delta KD}$ mice compared to control mice. Liver tissue sections showed evidence of liver damage following α-GalCer stimulation at day 3. The livers of *Map3k1*$^{\Delta KD}$ mice showed a significant increase in lymphocyte infiltration (Fig. 13B). The role of *Map3ks* were also determined in day 3 glycolipid stimulated PBMC. There were significantly reduced iNKT cell numbers in *Map3k1*$^{\Delta KD}$ PBMC compared to control mice (Fig. 13C) therefore showing *Map3k1* control iNKT cell homeostatsis and expansion in PBMC.

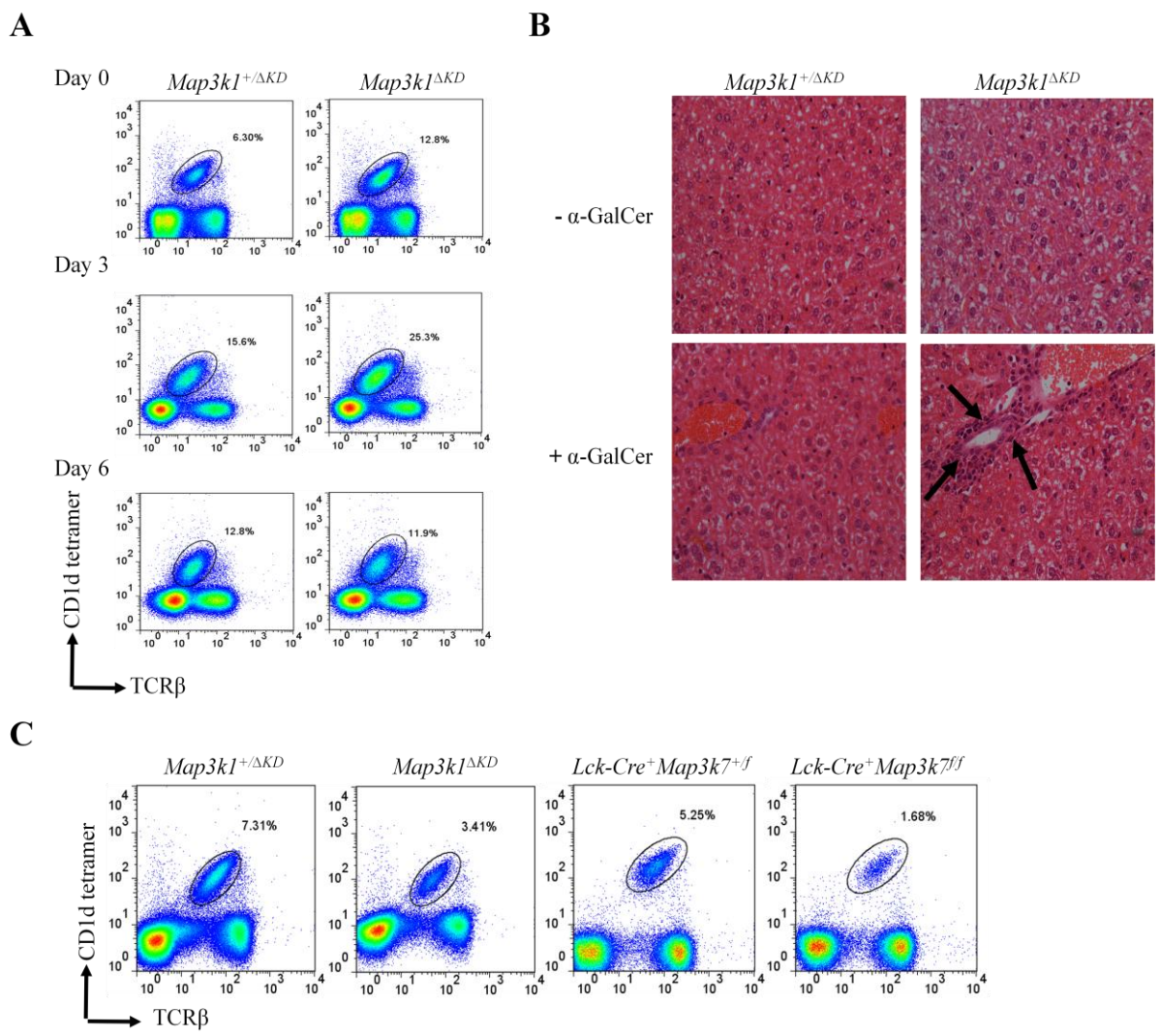

Fig 13. *Map3k*-dependent regulation of iNKT cell expansion within the liver and PBMC.
Liver cells were harvested at days 0, 3 and 6 from *Map3k1*$^{+/\Delta KD}$ and *Map3k1*$^{\Delta KD}$ mice that were i.p. immunized with α-GalCer over a 6 day time course as stated in the material and methods. (A) Liver cells were stained with CD1d tetramer and anti-TCRβ antibody and analyzed by flow cytometry as stated in the materials and methods. An expansion of iNKT cells in the liver with a peak response on day 3, followed by a steep decline in the number of iNKT cells to unstimulated levels by day 6 is seen. Data was representative of 3 mice per group from 3 independent experiments. (B) Representative H&E stained liver sections were prepared from unstimulated (upper panels) and 3 day α-GalCer stimulated (lower panels) control and *Map3k1*$^{\Delta KD}$ mice (original magnification x40). The livers of *Map3k1*$^{\Delta KD}$ mice showed a significant increase in lymphocyte infiltration at a vessel as indicated by arrows. Data was representative of 3 independent experiments. (C) PBMC from 3 day α-GalCer stimulated *Map3k1*$^{+/\Delta KD}$ and *Map3k1*$^{\Delta KD}$ mice were stained with CD1d tetramer and anti-TCRβ antibody and analyzed using flow cytometry. Reduced iNKT cell numbers in *Map3k1*$^{\Delta KD}$ PBMC compared to control mice was seen. Data was representative of 3 independent experiments.

Role of *Map3k1* in germinal center formation

Map3k1$^{+/\Delta KD}$ and *Map3k1*$^{\Delta KD}$ mice were immunized with KLH over a 12 day period. Germinal center formation was analyzed by using Gl-7, a marker for germinal center B cells and B220 a marker for B cells. Spleens from *Map3k1*$^{+/\Delta KD}$ mice had a larger population of activated B cells positive for the GL7 marker compared to *Map3k1*$^{\Delta KD}$ mice (Fig. 14). This therefore could suggest that mice lacking the activity of the kinase MEKK1 have defective germinal center formation.

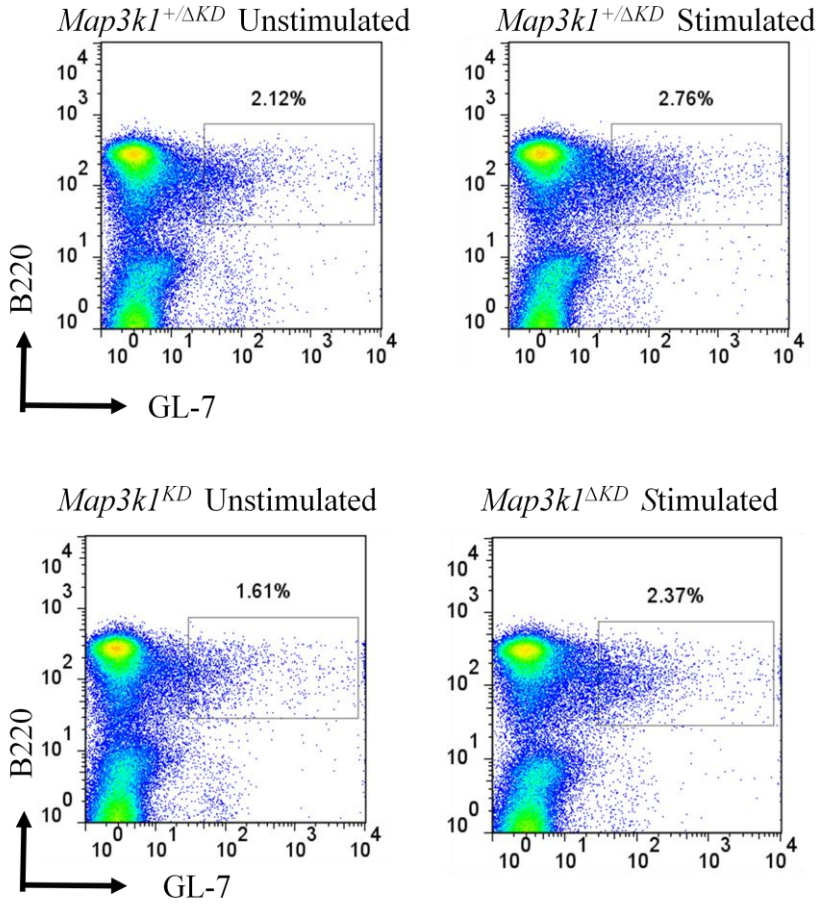

Fig 14. B cell stimulation in *Map3k1*$^{+/\Delta KD}$ mice
i.p. injections of KLH were administered to *Map3k1*$^{\Delta KD}$ and *Map3k1*$^{+/\Delta KD}$ mice over a 12 day time period. Splenocytes were harvested at day 10, and stained with B cell markers GL7 and B220 and analyzed using flow cytometry. Spleens from *Map3k1*$^{+/\Delta KD}$ mice stimulated with KLH had a larger number of B cells positive for the GL7 marker compared to spleens from *Map3k1*$^{\Delta KD}$ mice stimulated with KLH. Data was representative of 3 mice per group.

IFN-γ and IL-4 production in *Map3k1$^{\Delta KD}$* and *Map3k1$^{+/\Delta KD}$* mice

Due to the defect in germinal center formation in *Map3k1$^{\Delta KD}$* mice, IFN-γ and IL-4 production was analyzed in *Map3k1$^{+/\Delta KD}$* and *Map3k1$^{\Delta KD}$* mice immunized with KLH over a 12 day period by flow cytometry (Fig. 15). No significant difference in the percentage of IFN-γ^{+} and IL-4^{+} from CD3^{+} T cells between *Map3k1$^{+/\Delta KD}$* and *Map3k1$^{\Delta KD}$* mice was observed. This could suggest that the defect in germinal center formation in *Map3k1$^{\Delta KD}$* mice is due to a knockout of MEKK1 in B cells and not from a T cell defect.

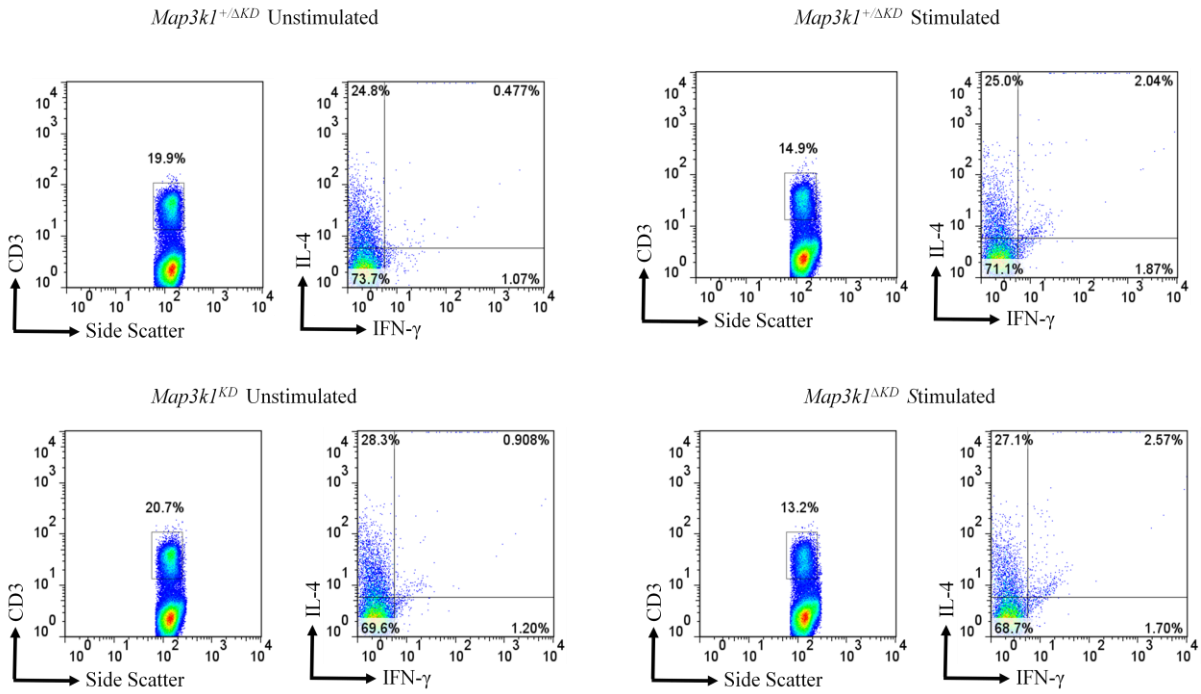

Fig 15. IFN-γ and IL-4 production in *Map3k1$^{\Delta KD}$* and *Map3k1$^{+/\Delta KD}$* mice
i.p. injections of KLH were administered to *Map3k1$^{\Delta KD}$* and *Map3k1$^{+/\Delta KD}$* mice over a 12 day time period. Splenocytes were harvested at day 10, and stained with anti-CD3, anti-IFN-γ and anti-IL-4 antibodies and analyzed using flow cytometry. No significant difference was seen in the percentage of IL-4 and IFN-γ positive cells produced from the CD3^{+} fraction by *Map3k1$^{\Delta KD}$* and *Map3k1$^{+/\Delta KD}$* mice. Data was representative of 3 mice per group.

Discussion

In this research study, we have investigated the molecular roles of *Map3k1* and *Map3k7* in relation to iNKT cells (Fig.16). We observe that no iNKT developmental defects are present in *Map3k1*$^{\Delta KD}$ or *Lck-Cre*$^{+}$*Map3k7*$^{f/f}$ mice. We see that there appears to be a defect in iNKT cell expansion in *Map3k1*$^{\Delta KD}$ mice, to asses this defect, microarray genetic profiling was performed to understand the molecular basis of the iNKT cell defect. p27 a cell cycle inhibitor provides an explanation for the hypoproliferation seen in *Map3k1*$^{\Delta KD}$. An upregulated expression of Th17 related genes *Rorc*, *Mmp9* and *Il17rb* in *Map3k1*$^{\Delta KD}$ iNKT cells has also been identified suggesting an association between the Th17 differentiation pathway and the *Map3k1*$^{\Delta KD}$ iNKT cells Furthermore, enhanced expression of IL-17 and IL-1 cytokines could account for the enhanced liver damage observed in *Map3k1*$^{\Delta KD}$mice.

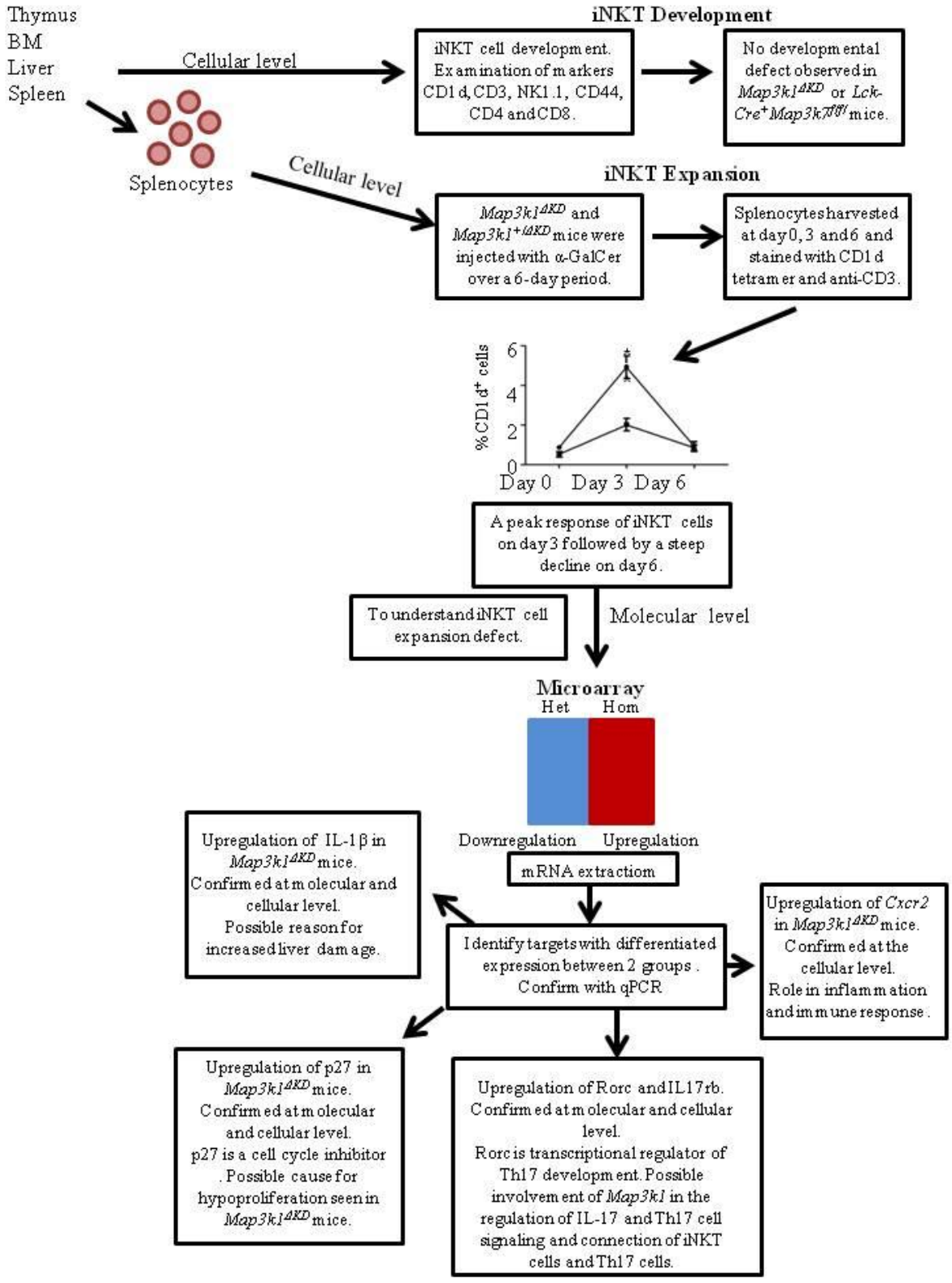

Fig 16. Methodology of our research and results. Detailed schematic diagram outlining the research performed in this study, and the overall results.

It has been demonstrated that disruption of *Map3k1* and *Map3k7* genes does not cause a change to iNKT cell development. However *Map3k1*$^{\Delta KD}$, mice that have been injected with α-GalCer, show reduced number of iNKT cell numbers on day 3 of a 6 day time course, giving evidence to defective iNKT expansion. In contrast, there is elevated iNKT expansion in *Lck-Cre*$^{+}$*Map3k1*$^{f/f}$ compared to control mice at day 3. This therefore demonstrates *Map3k1* and *Map3k7* regulate iNKT expansion by distinct mechanisms. Studies have shown that *in vivo* stimulation of iNKT cells with α-GalCer shows a disappearance of cells within 3-12 hours and reappearance 24-48 hours later. Expansion of up to 10-fold results in a maximal number of iNKT cells on day 3 followed by a decrease in cell numbers at day 6-9 to the same level as before stimulation. It is thought that it is a downregulation of TCR and NK1.1 that is the cause if iNKT disappearance. Others report that a fall in iNKT cell number after stimulation is caused by apoptosis mediated by Bim and classical Fas-FasL mediated activated induced cell death (Ansari et al., 2010).

MAP3Ks are associated with several signaling pathway in cell types other than iNKT cells. *Map3k7* has a role in NF-κB, p38 and JNK signaling pathways and cytokine production in a cell type specific manner where it is found to be a negative regulator in neutrophils, however it is an important positive regulator in macrophages and fibroblasts (Ajibade et al., 2012). Several signaling pathways are involved in the regulation and development, maturation and survival of NKT cells including SLAM:SAP:Fyn, calcineurin:NFAT:Egr2, NIK:RelB and PKCΘ:NF-κB pathways (Bendelac et al., 2007; Griewank et al., 2007; Lazarevic et al., 2009; Sivakumar et al., 2003). Microarray gene expression and bioinformatics analysis and phosphor-MAPK FACS analysis both show that *Map3k1* plays a role in p38 MAPK signaling in iNKT cells.

To understand the molecular basis of the *Map3k1*$^{\Delta KD}$ iNKT cell defect in long term expansion, microarray gene expression profiles between *Map3k1*$^{+/\Delta KD}$ and *Map3k1*$^{\Delta KD}$ iNKT cells have been compared. One of the screened hits, p27 a cell cycle inhibitor display elevated expression in *Map3k1*$^{\Delta KD}$ iNKT cells compared to *Map3k1*$^{+/\Delta KD}$ mice. This therefore offers an explanation for the iNKT cell hypoproliferation seen in *Map3k1*$^{\Delta KD}$ mice. p27 is an inhibitor of cyclin dependent kinase (CDK) involved in the regulation of the cell cycle. CDKs control cell cycle progression that are

activated by cyclin binding and inhibited by CDK inhibitors. CDKs regulate checkpoints that combine mitogenic and growth inhibitory signals, coordinating cell cycle transitions. Passage from the G_1 phase to the S phase is regulated by the activities of cyclin D1/CDK4, cyclin E/CDK2 and cyclin A/CDK2 complexes. Cyclin B/CDK1 regulates the G_2 phase -M transition. p27 has a negative effect on the activities of cyclin E/CDK2 and cyclin A/CDK2, it activates cyclin D/CDK complexes. In proliferating cells p27 is commonly bound to cyclin D/CDKs, whereas in G_1 arrested cells p27 is found in complexes with cyclin E/CDK2. Therefore the competition for p27 between cyclin D/CDKs and cyclin E/CDK2 complexes seem to be essential for cell cycle progression as cyclin D/CDKs can sequester p27 from the cyclone E/CDK2 complex and favour progression into the S phase (Chiarle et al., 2001). It is a reasonable assumption that in our *Map3k1*$^{\Delta KD}$ cells which have high levels of p27 expression, p27 would be complexed with cyclin E/CDK2. This would explain the hypoproliferation in *Map3k1*$^{\Delta KD}$cells. p27 and cyclin D leads to proliferation of cells, whereas p27 and cyclin E leads to cell arrest.

A second subset of screened hits from the *Map3k1*$^{\Delta KD}$ iNKT microarray are IL-17 and Th17 cell signaling genes (*Rorc, IL17rb and Mmp9*), and this exhibits the involvement of *Map3k1* in the regulation of IL-17 and Th17 cell signaling. *Map3k1*$^{\Delta KD}$ iNKT cells overproduce IL-17 which correlates with the upregulated expression of Th17 related microarray hits. *Rorc* is downstream to phosphorylated STAT3 in Th17 cells; however there was downregulated expression of phosphorylated STAT3 in *Map3k1*$^{\Delta KD}$ iNKT cells which is in contradiction with the upregulated expression of *Rorc* in *Map3k1*$^{\Delta KD}$ iNKT cells. A possible explanation for this is that *Rorc* is constitutively expressed in NKT cells (Rachitskaya et al., 2008), and therefore phosphorylated STAT3 is not necessary for *Rorc* expression under these circumstances. *Rorc* is essential for the development of secondary lymphoid tissues; it is also involved in lineage specification of uncommitted $CD4^+$ T helper cells into Th17 cells. *Map3k1:MAPK* signaling is a negative regulator of constitutive *Rorc* expression in iNKT cells. A distinct IL-17 producing iNKT subset (known as iNKTH17) has recently been identified (Michel et al., 2007; Michel et al., 2008). 2.5% of iNKT cells in the spleen were $Rorc^+$

and when stimulated with α-GalCer produced high levels of IL-17. This indicates that *Rorc* expression is an important marker for identifying IL-17 producing iNKT cells (Michel et al., 2008).

Th17 cells play a role in the onset and progression of some forms of cell mediated autoimmunity. Differentiation of Th17 cells can take place in the presence of particular cytokine combinations including TGF-β and IL-6 or TGF-β and IL-21. Th17 cells also have the ability to upregulate the IL-23 receptor, IL-23 is important for Th17 expansion and maintenance. RORγt is the transcriptional regulator if Th17 development and in its absence Th17 cells fail to develop, an overexpression of RORγt enhances Th17 development (Coquet et al., 2008). It has been found that iNKT cells that lack the NK1.1 marker secrete high concentrations of IL-17 and it has recently been demonstrated that NKT cells that express IL-23R secrete IL-17 following stimulation with anti-CD3 and IL-23. Furthermore, NKT cells can secrete IL-17 in response to the ligand α-GalCer (Mills, 2008). Rapid IL-17 release by iNKT cells that lack NK1.1 may have important physiological consequences. Th17 cells are considered as being the main source of IL-17 during immune responses, Th17 cells are differentiated effector CD4 T cells that develop from naive CD4 T cells in the presence of cytokines over a matter of days. NKT cells however can produce IL-17 within three hours and are therefore an important primary source of this proinflammatory cytokine (Coquet et al., 2008).

In *Map3k1*$^{\Delta KD}$ mice there is increased in iNKT cell infiltration in the liver and a higher amount of liver damage compared with *Map3k1*$^{+/\Delta KD}$. These observations suggest that the processes underlying iNKT population homeostasis and expansion in the liver are distinct. An elevated amount of circulating IL-17 and IL-1β in *Map3k1*$^{\Delta KD}$ mice can provide an explanation for the increased iNKT cell infiltration into the liver (Hammerich et al., 2011; Lafdil et al., 2010; Ye et al., 2011). This is supported by the iNKT microarray analysis in the increased expression of Th17 and IL-1β related genes (*Il17rb, Rorc, Ilr2 and Il1f9*) at the mRNA level in *Map3k1*$^{\Delta KD}$ iNKT cells. Both IL-17 and IL-1β have been previously shown to have pro-inflammatory roles in liver damage (Watarai et al., 2012). It has also been shown that stimulation with IL-17 induces the expression of several inflammation associated genes, including chemokines and C-reactive protein in primary hepatocytes (Patel et al., 2007; Sparna et al., 2010). Furthermore a clinical study showed that serum levels of *IL-1β*, *IL-6*, *TNF-α*, *IFN-α* and

C-Reactive Protein were elevated in patients with chronic liver diseases (Tilg et al., 1992). Future research using *Map3k* transgenic mice as an experimental approach will help to explain T cell-dependent inflammatory mechanisms in the liver further.

Further in depth research based on microarray analysis of *Map3k1*$^{\Delta KD}$ Th17 cells may reveal differentially-regulated genes that are common to both iNKT and Th17 cells, which would clarify the mechanisms that crosslink in those two distinct cell types. It would be interesting to study a Th17 related disease such as experimental autoimmune encephalomyelitis (EAE), which is a murine model of multiple sclerosis (Piccio et al., 2013), and investigate the possible relationship between Th17 cells and iNKT cells at the cellular, protein and molecular levels to identify the involvement of critical molecules. Moreover, work carried out in *Map3k1/flox-Lck-Cre* will silence the *Map3k1*gene specifically in the T-cell lineage in contrast to the germline and will further identify MAPK signaling molecules that play a role in iNKT and Th17 development.

There is a smaller number of activated B cells from the GL-7 marker in *Map3k1*$^{\Delta KD}$ mice compared to *Map3k1*$^{+/\Delta KD}$ mice suggesting that there is a defect in germinal center formation. This defect could be explained by the possible contribution of MEKK1 in other cell types (T cells and DC's) to germinal center formation as indicated by a previous research study (Gallagher et al., 2007). However we did not find any obvious defect in the ability of *Map3k1*$^{\Delta KD}$ $CD3^+$ T cells to induce production of cytokines IFN-γ and IL-4, we can therefore assume that mice lacking activity of MEKK1 in B cells is the cause of the germinal center defect. It has been previously observed that the absence of MEKK1 catalytic activity resulted in a considerable defect in germinal center formation and the production of TD-antigen specific antibodies.

This work shows preliminary results on KLH-stimulated mice. More work is required in the study of B cells in *Map3k1*/*CD19-Cre* mice, identifying how the effect of silencing the *Map3k1* gene in B cells will influence MAPK signaling and pinpoint the mechanisms involved. It would be interesting to investigate the expression of cytokines at a cellular level between mutant and control mice. Conformation of cytokine expression could be carried out by ELISA by measuring protein secretion

levels. Furthermore, investigating how the protein expression of JNK, ERK and p38 differs in *Map3k1*^{flox} versus control mice will lead to the greater understanding of the mechanisms of MAPK signaling in B cells. Further research in B, T cell and iNKT cells could lead to the development of potential therapies in autoimmune diseases.

Limitations

Mechanisms in mice may be different from those taking place in humans, this may make it difficult to correlate the results in human subjects in order to develop efficient therapies.

We have tried to create an artificial system that mimics as closely as possible the stimulation happening in the human body. However the stimulation conditions used (stimulation with α-GalCer) in the study to induce iNKT production may vary to some degree in a physiological context.

References

Book

Murphy, K. (2011). Janeway's Immunobiology 8th Edition (Garland Science).

Articles

Ajibade, A.A., Wang, Q., Cui, J., Zou, J., Xia, X., Wang, M., Tong, Y., Hui, W., Liu, D., Su, B., *et al.* (2012). TAK1 negatively regulates NF-kappaB and p38 MAP kinase activation in Gr-1+CD11b+ neutrophils. Immunity *36*, 43-54.

Ansari, A.W., Temblay, J.N., Alyahya, S.H., and Ashton-Rickardt, P.G. (2010). Serine protease inhibitor 6 protects iNKT cells from self-inflicted damage. Journal of immunology (Baltimore, Md. : 1950) *185*, 877-883.

Aouadi, M., Binetruy, B., Caron, L., Le Marchand-Brustel, Y., and Bost, F. (2006). Role of MAPKs in development and differentiation: lessons from knockout mice. Biochimie *88*, 1091-1098.

Arana-Argaez, V.E., Delgado-Rizo, V., Pizano-Martinez, O.E., Martinez-Garcia, E.A., Martin-Marquez, B.T., Munoz-Gomez, A., Petri, M.H., Armendariz-Borunda, J., Espinosa-Ramirez, G., Zuniga-Tamayo, D.A., *et al.* (2010). Inhibitors of MAPK pathway ERK1/2 or p38 prevent the IL-1{beta}-induced up-regulation of SRP72 autoantigen in Jurkat cells. The Journal of biological chemistry *285*, 32824-32833.

Ayyoub, M., Deknuydt, F., Raimbaud, I., Dousset, C., Leveque, L., Bioley, G., and Valmori, D. (2009). Human memory FOXP3+ Tregs secrete IL-17 ex vivo and constitutively express the T(H)17 lineage-specific transcription factor RORgamma t. Proceedings of the National Academy of Sciences of the United States of America *106*, 8635-8640.

Bendelac, A., Savage, P.B., and Teyton, L. (2007). The biology of NKT cells. Annual review of immunology *25*, 297-336.

Berland, R., and Wortis, H.H. (2002). Origins and functions of B-1 cells with notes on the role of CD5. Annual review of immunology *20*, 253-300.

Bouaziz, J.D., Yanaba, K., and Tedder, T.F. (2008). Regulatory B cells as inhibitors of immune responses and inflammation. Immunological reviews *224*, 201-214.

Chen, Z., Laurence, A., Kanno, Y., Pacher-Zavisin, M., Zhu, B.M., Tato, C., Yoshimura, A., Hennighausen, L., and O'Shea, J.J. (2006). Selective regulatory function of Socs3 in the formation of IL-17-secreting T cells. Proceedings of the National Academy of Sciences of the United States of America *103*, 8137-8142.

Chiarle, R., Pagano, M., and Inghirami, G. (2001). The cyclin dependent kinase inhibitor p27 and its prognostic role in breast cancer. Breast cancer research : BCR *3*, 91-94.

Coquet, J.M., Chakravarti, S., Kyparissoudis, K., McNab, F.W., Pitt, L.A., McKenzie, B.S., Berzins, S.P., Smyth, M.J., and Godfrey, D.I. (2008). Diverse cytokine production by NKT cell subsets and identification of an IL-17-producing CD4-NK1.1- NKT cell population. Proceedings of the National Academy of Sciences of the United States of America *105*, 11287-11292.

Gaffen, S.L. (2009). Structure and signalling in the IL-17 receptor family. Nature reviews. Immunology *9*, 556-567.

Gallagher, E., Enzler, T., Matsuzawa, A., Anzelon-Mills, A., Otero, D., Holzer, R., Janssen, E., Gao, M., and Karin, M. (2007). Kinase MEKK1 is required for CD40-dependent activation of the kinases Jnk and p38, germinal center formation, B cell proliferation and antibody production. Nature immunology *8*, 57-63.

Gapin, L., Matsuda, J.L., Surh, C.D., and Kronenberg, M. (2001). NKT cells derive from double-positive thymocytes that are positively selected by CD1d. Nature immunology *2*, 971-978.

Gray, D., Gray, M., and Barr, T. (2007). Innate responses of B cells. European journal of immunology *37*, 3304-3310.

Griewank, K., Borowski, C., Rietdijk, S., Wang, N., Julien, A., Wei, D.G., Mamchak, A.A., Terhorst, C., and Bendelac, A. (2007). Homotypic interactions mediated by Slamf1 and Slamf6 receptors control NKT cell lineage development. Immunity *27*, 751-762.

Hammerich, L., Heymann, F., and Tacke, F. (2011). Role of IL-17 and Th17 cells in liver diseases. Clinical & developmental immunology *2011*, 345803.
Inoue, T., Boyle, D.L., Corr, M., Hammaker, D., Davis, R.J., Flavell, R.A., and Firestein, G.S. (2006). Mitogen-activated protein kinase kinase 3 is a pivotal pathway regulating p38 activation in inflammatory arthritis. Proceedings of the National Academy of Sciences of the United States of America *103*, 5484-5489.
Ivanov, II, McKenzie, B.S., Zhou, L., Tadokoro, C.E., Lepelley, A., Lafaille, J.J., Cua, D.J., and Littman, D.R. (2006). The orphan nuclear receptor RORgammat directs the differentiation program of proinflammatory IL-17+ T helper cells. Cell *126*, 1121-1133.
Karin, M., and Gallagher, E. (2005). From JNK to pay dirt: jun kinases, their biochemistry, physiology and clinical importance. IUBMB life *57*, 283-295.
Kiyokawa, H., Kineman, R.D., Manova-Todorova, K.O., Soares, V.C., Hoffman, E.S., Ono, M., Khanam, D., Hayday, A.C., Frohman, L.A., and Koff, A. (1996). Enhanced growth of mice lacking the cyclin-dependent kinase inhibitor function of p27(Kip1). Cell *85*, 721-732.
Lafdil, F., Miller, A.M., Ki, S.H., and Gao, B. (2010). Th17 cells and their associated cytokines in liver diseases. Cellular & molecular immunology *7*, 250-254.
Lazarevic, V., Zullo, A.J., Schweitzer, M.N., Staton, T.L., Gallo, E.M., Crabtree, G.R., and Glimcher, L.H. (2009). The gene encoding early growth response 2, a target of the transcription factor NFAT, is required for the development and maturation of natural killer T cells. Nature immunology *10*, 306-313.
Matsuda, J.L., Mallevaey, T., Scott-Browne, J., and Gapin, L. (2008). CD1d-restricted iNKT cells, the 'Swiss-Army knife' of the immune system. Current opinion in immunology *20*, 358-368.
Matsuzawa, A., Tseng, P.H., Vallabhapurapu, S., Luo, J.L., Zhang, W., Wang, H., Vignali, D.A., Gallagher, E., and Karin, M. (2008). Essential cytoplasmic translocation of a cytokine receptor-assembled signaling complex. Science (New York, N.Y.) *321*, 663-668.
Mauri, C. (2010). Regulation of immunity and autoimmunity by B cells. Current opinion in immunology *22*, 761-767.
Michel, M.L., Keller, A.C., Paget, C., Fujio, M., Trottein, F., Savage, P.B., Wong, C.H., Schneider, E., Dy, M., and Leite-de-Moraes, M.C. (2007). Identification of an IL-17-producing NK1.1(neg) iNKT cell population involved in airway neutrophilia. The Journal of experimental medicine *204*, 995-1001.
Michel, M.L., Mendes-da-Cruz, D., Keller, A.C., Lochner, M., Schneider, E., Dy, M., Eberl, G., and Leite-de-Moraes, M.C. (2008). Critical role of ROR-gammat in a new thymic pathway leading to IL-17-producing invariant NKT cell differentiation. Proceedings of the National Academy of Sciences of the United States of America *105*, 19845-19850.
Mills, K.H. (2008). Induction, function and regulation of IL-17-producing T cells. European journal of immunology *38*, 2636-2649.
Miossec, P., and Kolls, J.K. (2012). Targeting IL-17 and TH17 cells in chronic inflammation. Nature reviews. Drug discovery *11*, 763-776.
Montecino-Rodriguez, E., Leathers, H., and Dorshkind, K. (2006). Identification of a B-1 B cell-specified progenitor. Nature immunology *7*, 293-301.
Ninomiya-Tsuji, J., Kishimoto, K., Hiyama, A., Inoue, J., Cao, Z., and Matsumoto, K. (1999). The kinase TAK1 can activate the NIK-I kappaB as well as the MAP kinase cascade in the IL-1 signalling pathway. Nature *398*, 252-256.
Novak, J., and Lehuen, A. (2011). Mechanism of regulation of autoimmunity by iNKT cells. Cytokine *53*, 263-270.
Ouyang, W., Kolls, J.K., and Zheng, Y. (2008). The biological functions of T helper 17 cell effector cytokines in inflammation. Immunity *28*, 454-467.
Patel, D.N., King, C.A., Bailey, S.R., Holt, J.W., Venkatachalam, K., Agrawal, A., Valente, A.J., and Chandrasekar, B. (2007). Interleukin-17 stimulates C-reactive protein expression in hepatocytes and smooth muscle cells via p38 MAPK and ERK1/2-dependent NF-kappaB and C/EBPbeta activation. The Journal of biological chemistry *282*, 27229-27238.
Pearson, G., Robinson, F., Beers Gibson, T., Xu, B.E., Karandikar, M., Berman, K., and Cobb, M.H. (2001). Mitogen-activated protein (MAP) kinase pathways: regulation and physiological functions. Endocrine reviews *22*, 153-183.

Piccio, L., Cantoni, C., Henderson, J.G., Hawiger, D., Ramsbottom, M., Mikesell, R., Ryu, J., Hsieh, C.S., Cremasco, V., Haynes, W., *et al.* (2013). Lack of adiponectin leads to increased lymphocyte activation and increased disease severity in a mouse model of multiple sclerosis. European journal of immunology.
Rachitskaya, A.V., Hansen, A.M., Horai, R., Li, Z., Villasmil, R., Luger, D., Nussenblatt, R.B., and Caspi, R.R. (2008). Cutting edge: NKT cells constitutively express IL-23 receptor and RORgammat and rapidly produce IL-17 upon receptor ligation in an IL-6-independent fashion. Journal of immunology (Baltimore, Md. : 1950) *180*, 5167-5171.
Rincon, M., and Davis, R.J. (2009). Regulation of the immune response by stress-activated protein kinases. Immunological reviews *228*, 212-224.
Sivakumar, V., Hammond, K.J., Howells, N., Pfeffer, K., and Weih, F. (2003). Differential requirement for Rel/nuclear factor kappa B family members in natural killer T cell development. The Journal of experimental medicine *197*, 1613-1621.
Sparna, T., Retey, J., Schmich, K., Albrecht, U., Naumann, K., Gretz, N., Fischer, H.P., Bode, J.G., and Merfort, I. (2010). Genome-wide comparison between IL-17 and combined TNF-alpha/IL-17 induced genes in primary murine hepatocytes. BMC genomics *11*, 226.
Tilg, H., Wilmer, A., Vogel, W., Herold, M., Nolchen, B., Judmaier, G., and Huber, C. (1992). Serum levels of cytokines in chronic liver diseases. Gastroenterology *103*, 264-274.
Veldhoen, M., Hocking, R.J., Atkins, C.J., Locksley, R.M., and Stockinger, B. (2006). TGFbeta in the context of an inflammatory cytokine milieu supports de novo differentiation of IL-17-producing T cells. Immunity *24*, 179-189.
Viau, M., and Zouali, M. (2005). B-lymphocytes, innate immunity, and autoimmunity. Clinical immunology (Orlando, Fla.) *114*, 17-26.
Wang, C., Deng, L., Hong, M., Akkaraju, G.R., Inoue, J., and Chen, Z.J. (2001). TAK1 is a ubiquitin-dependent kinase of MKK and IKK. Nature *412*, 346-351.
Watarai, H., Sekine-Kondo, E., Shigeura, T., Motomura, Y., Yasuda, T., Satoh, R., Yoshida, H., Kubo, M., Kawamoto, H., Koseki, H., and Taniguchi, M. (2012). Development and function of invariant natural killer T cells producing T(h)2- and T(h)17-cytokines. PLoS biology *10*, e1001255.
Wilson, N.J., Boniface, K., Chan, J.R., McKenzie, B.S., Blumenschein, W.M., Mattson, J.D., Basham, B., Smith, K., Chen, T., Morel, F., *et al.* (2007). Development, cytokine profile and function of human interleukin 17-producing helper T cells. Nature immunology *8*, 950-957.
Ye, C., Li, W.Y., Zheng, M.H., and Chen, Y.P. (2011). T-helper 17 cell: A distinctive cell in liver diseases. Hepatology research : the official journal of the Japan Society of Hepatology *41*, 22-29.
Zhou, L., and Littman, D.R. (2009). Transcriptional regulatory networks in Th17 cell differentiation. Current opinion in immunology *21*, 146-152.

Acknowledgements

I would like to thank Ewen Gallagher and Tesha Suddason for their valuable help and guidance throughout my master's thesis. I would also like to thank my family for the continuous support they have given me throughout my education.